Western and Central Pacific Fisheries Commission

SCIENTIFIC COMMITTEE
THIRTEENTH REGULAR SESSION

Rarotonga, Cook Islands
9 – 17 August 2017

Project 35: Age, growth and maturity of bigeye tuna
in the western and central Pacific Ocean

Farley J[1]., P. Eveson[1], K. Krusic-Golub[2], C. Sanchez[3], F. Roupsard[3], S. McKechnie[3], S. Nicol[34], B. Leroy[3], N. Smith[3] and S-K Chang[5]

[1] CSIRO Oceans & Atmosphere
[2] Fish Ageing Services Pty Ltd
[3] Pacific Community
[4] University of Canberra
[5] Institute of Marine Affairs, College of Marine Sciences, National Sun Yat-sen University

Project 35: Age, growth and maturity of bigeye tuna in the western and central Pacific Ocean

Jessica Farley[1], Paige Eveson[1], Kyne Krusic-Golub[2], Caroline Sanchez[3], Francois Roupsard[3], Sam McKechnie[3], Simon Nicol[3,4] , Bruno Leroy[3], Neville Smith[3], Shui-Kai Chang[5]

[1] CSIRO Oceans & Atmosphere

[2] Fish Ageing Services Pty Ltd

[3] Pacific Community

[4] University of Canberra

[5] Institute of Marine Affairs, College of Marine Sciences, National Sun Yat-sen University

Acknowledgements

Contents

1   Executive summary

This paper describes a regional study of bigeye tuna population biology. The objectives were to estimate the growth of bigeye in the western and central Pacific Ocean (WCPO) and examine spatial variation in growth, for application in regional stock assessment models. In addition, the project aimed to determine the reproductive status and maturity-at-length/age of bigeye in the WCPO.

Validated annual ageing protocols for otoliths were followed in this study, and counts of opaque zones were obtained for 1039 fish caught between 2013 and 2016. A decimal age was estimated using the count of opaque zones, birth date, capture date and the state of completion of the marginal increment (edge classification) of the otolith. Annual ages ranged from 0.25 to 13.67 years. In addition, (presumed) daily age estimates were obtained for 100 fish ranging from 153-857 days (transverse and longitudinal sections combined), although sectioned otoliths were difficult to interpret beyond 300 zones.

The results from fitting VB models to the age data suggest that growth does not vary substantially between males and females, or between regions 3 and 4 of the stock assessment (western equatorial Pacific). However, exploratory work using length-at-age estimates from all regions suggests that growth of bigeye varies spatially in the WCPO. In general, length-at-age is above average at the westernmost (<140°E) and easternmost (>205°E) longitudes, and below average within the central longitudes (140-205°E). Analysis of additional otoliths from all areas and from the full size range of fish over a larger number of years is required to fully explore spatial variation in growth of bigeye across the Pacific.

Standard reproductive classification criteria for tuna reproductive biology was used to assess the development phase of 343 females caught between 2011 and 2016. Spawning capable females were only found between 12°N and 12°S and between 137°E and 130°W. Spawning occurred year-round with indicative peaks in activity in May and October. Spawning capable females occurred in SSTs between 27.7 and 30.3°C, but were in highest relative abundance at SSTs between 28 and 29°C. A large number regressing and regenerating females were caught in SSTs ≥27°C demonstrating that not all females are reproductively active at these temperatures.

Logistic models fit to the maturity data suggest that maturity-at-length/age differed slightly between regions 3 and 4 of the stock assessment. Similar to the growth results, exploratory work using maturity data from all regions suggests that maturity of bigeye varies spatially in the WCPO. The proportion of mature females at a given length or age tended to increase from the southwest to the northeast of the study region. However, analysis of additional ovaries is required to more comprehensively investigate regional variation in maturity and account for inter-annual variation.

2   Introduction

The Western and Central Pacific Fishery Commission (WCPFC), through Project 35, has conducted biological studies on tuna and billfish in the western and central Pacific Ocean (WCPO) to address uncertainties in life history. Accurate life-history parameters are required for robust stock assessments and management advice. In 2008, the Western and Central Pacific Fisheries Commission (WCPFC) endorsed a "Comprehensive Research Plan on Pacific-wide Bigeye Growth and Reproductive Biology" and supported a pilot project to determine the sampling requirements for implementing this study (Project 35). In 2009, a work plan for the project was finalised and in 2011 a pilot project was completed (Nicol et al. 2011). Preliminary estimates of bigeye age, growth and maturity were obtained for region 3 and 4 (western equatorial Pacific) and the sensitivity of the bigeye stock assessment to these estimates was evaluated (Nicol et al. 2011). After reviewing the pilot project, the WCPFC supported the continuation of the sampling and analysis program to gain a better understanding of bigeye age and maturity. By 2013, tissue banks were established at SPC and CSIRO to archive the biological material collected by Pacific Island Countries and Territories across the region under the project.

In 2014, the WCPFC endorsed the 'analysis phase' of Project 35 which required specialised analysis of otoliths and ovaries to estimate length- and maturity-at-age of bigeye tuna. The Pacific Community (SPC) Oceanic Fisheries Program (OFP) and the CSIRO have implemented this most recent analytical component of Project 35. The purpose of this project component was to estimate the growth of bigeye tuna in the WCPO and examine spatial variation in growth, for application in regional stock assessment models. In addition, the research aimed to determine the reproductive status and maturity-at-length of bigeye tuna in the WCPO.

3 Methods

3.1 Age and growth

3.1.1 Study material

A total of 1494 otoliths collected between 2013 and 2016 were available for analysis in the WCPFC tuna tissue bank. Of these, 1003 were selected for annual ageing. The majority (86.7%) were collected in the equatorial regions 3 and 4 of the bigeye stock assessment and were generally collected from longline fisheries in the region. To examine potential spatial variation in growth, all available otoliths from outside these regions were selected first (n=183) (Fig. 1). The remaining 820 otoliths were selected from regions 3 and 4; selection was based on size of fish (length stratified sampling scheme rather than random sampling) to ensure enough age estimates were

obtained from length classes where sample sizes were small. All otoliths from fish <88 cm and >123 cm FL were selected for ageing. An additional 52 otoliths were obtained from fish caught by the Chinese Taipei longline fishery in 2015. Overall, fish selected for annual ranged from 28-192 cm fork length (FL) (Fig. 1). Sex was known for 900 fish.
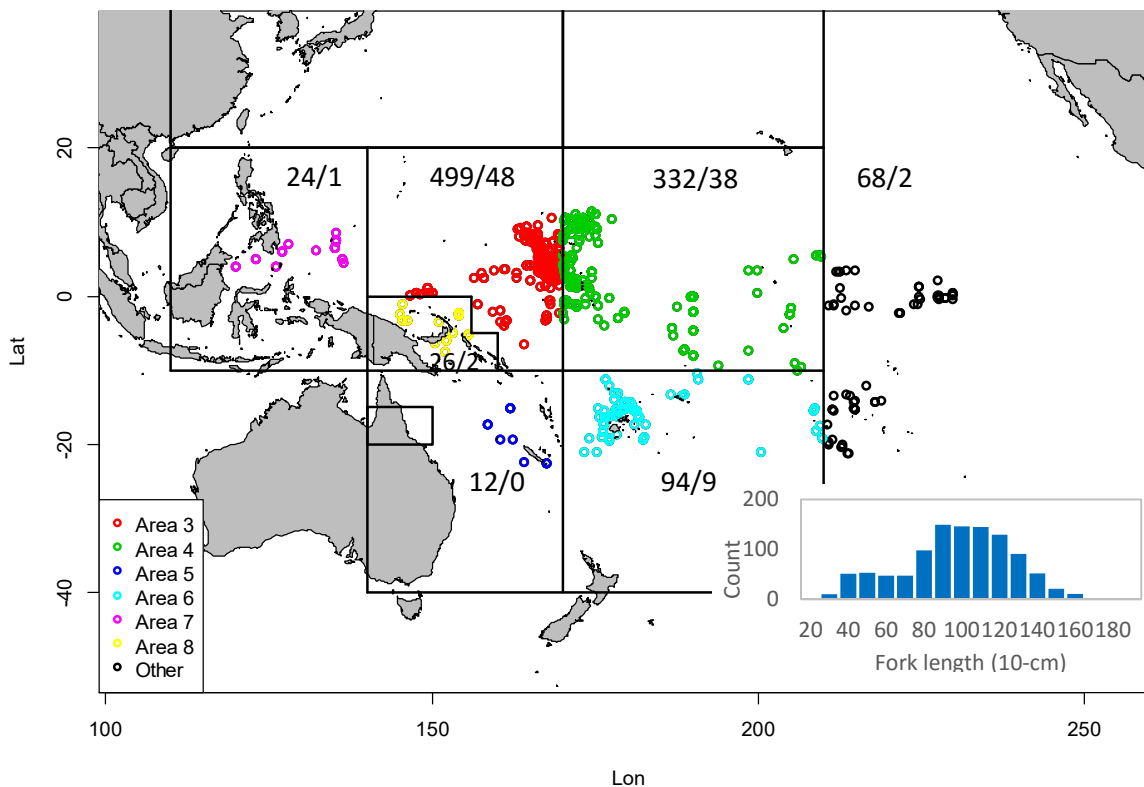
Figure 1. Map of the otolith sampling locations. Different colours represent different WCPFC stock assessment regions for bigeye tuna. The number of bigeye selected for age estimation (annual/daily) by region is indicated; n=1055/100. Longitude shown in degrees east. Length frequency of bigeye tuna selected for annual ageing is shown in inset.

3.1.2 Annual age estimation

The otoliths were weighed to the nearest 0.001 g (if whole) and sent to Fish Ageing Services Pty Ltd (FAS) for sectioning and reading. Transverse sections of the otoliths were prepared following the methods outlined in Anon (2002). Otoliths were embedded in clear casting polyester resin and four or five serial sections 300 μm thick were cut from each otolith (around the primordium). Sections from each sample were cleaned, dried and mounted on glass microscope slides (50 × 76 mm) with resin. Sections were then covered with further resin and two glass coverslips (22 × 60 mm) were placed side by side.

All preparations were viewed once by the primary reader, using a dissecting microscope and transmitted light, before undertaking the first read. For calibration purposes, an ageing reference set (n=50 sectioned otoliths) was also read prior to first reading. Each otolith was then read twice

following the validated method developed by Clear *et al*. (2000) and Farley *et al*. (2006), and a final age assigned. Opaque zones were counted along a transect that ran from the first inflection point on the otolith to the edge of the otolith (see Appendix A). An opaque zone on the margin was only counted if it was fully formed. A customised image analysis system was used to measure the distance between the first inflection to the distal edge of each of the manually marked opaque zones, and to the edge of the otolith. A single jpg image of the section was also captured which indicated the positions of the marked zones.

Opaque zones at the terminal edge of the otolith were counted only if some translucent material was evident after the opaque zone.

A confidence score was assigned to each reading as:

0. No section

1. No pattern obvious – unreadable

2. Pattern present – unsure with age estimate

3. Good pattern present – slightly unsure in some areas

4. Good pattern – confident with age estimate

5. No doubt

A confidence score of 0 (no section) indicates that either the preparation failed or the otolith was not suitable for sectioning (broken).

The edge of each sectioned otolith was classified as either:

1. Narrow – new opaque zone forming on the edge (mostly or fully complete).

2. Intermediate – narrow translucent zone must be complete around the edge.

3. Wide – wide translucent zone almost complete.

All readings were conducted without reference to the size of the fish, date of capture, or to previous readings.

3.1.3 Precision and bias

To examine precision, 10% of the sectioned otoliths were read by a second reader (CSIRO) using the protocols described above. Again, for calibration purposes, an ageing reference set (n=50 sectioned otoliths) was read by the second reader prior to reading the otoliths from this study. The precision of readings (intra- and inter-reader consistency) was assumed using the coefficient of variation (CV) (Chang 1982). Age bias and age difference plots were also used to examine differences between readers.

3.1.4 Marginal increment and edge type analysis

Marginal increment and edge type analyses were undertaken to examine monthly variation in zone formation (Campana 2001). For otoliths with two or more opaque zones, the marginal increment ratio (MIR) was calculated as the distance from the distal edge of the last opaque zone to

the edge of the otolith (marginal increment), as a percentage of the previous increment. For edge type analysis, the proportion of otoliths with wide, intermediate and narrow edges (see section 2.1.2) was examined by month. It was necessary to pool data across years due to low sample sizes.

3.1.5 Daily age estimation

Otoliths from 100 fish between 42 and 120 cm FL were selected for preparation of daily ageing (Fig. 1). All otoliths were sent to FAS for sectioning and reading. Transverse sections were prepared for 30 otoliths (56-118 cm) and longitudinal sections were prepared for the remaining 70 otoliths (42-119 cm). The otoliths were sectioned following the methods outlined in Williams *et al.* (2013) and the number of visible microincrements was counted from the primordium to the terminal edge of the section under high magnification on a compound microscope.

The counts of microincrements on the otoliths sectioned on the transverse plane were used to confirm the location of the first 1-2 annual opaque growth zones. When present, the distance from the inflection point to the 365th and 730th increments and to the edge of the otolith was measured for otoliths sectioned on the transverse plane.

The counts of microincrements on the otoliths sectioned on the longitudinal plane were used to (i) examine the variation in back-calculated birth date; (ii) compare daily and annual age estimates from the same fish to investigate the method of assigning fish to their correct age-classes; and (iii) obtain estimates of length at (daily) age.

3.1.6 Decimal age algorithm

A decimal age was calculated using the count of (annual) opaque zones, an assumed birth date, otolith edge classification, and date of capture. In summary:

1. After examining several options, we assumed a birth date of 1 July. This date was the best at keeping fish from the same cohort "together" and did not result in negative ages.

2. Based on marginal increment and edge type analysis (see section 4.1.3), we assumed that opaque zones are completed in the period between April and September, and used 1 July as the point for adjusting the counts of opaque zones.

3. We then assumed all fish caught in October to March had completed an opaque zone since their last birthday. Therefore, the opaque zone count adjustment was 0 for all fish irrespective of edge classification (Table 1).

4. It was not known whether fish caught in April to September (increment formation period) had completed an opaque zone since their last birthday. For these fish, we used the date of capture and otolith edge classification (see section 3.1.2) to adjust the count of opaque zones following the criteria presented in Table 1.

The decimal age was calculated using the following algorithm: $a = (n + b) + r/365$

Where a is the decimal age, n the count, b the count adjustment (from Table 1), and r the day of capture (expressed as number of days since the assumed birth date of 1 July).

Table 1. Opaque zone count adjustment based on capture month (columns) and edge classification (rows).

EDGE CLASSIFICATION	OCTOBER TO MARCH	APRIL TO JUNE	JULY TO SEPTEMBER
Wide or Intermediate	0	0	+1
Narrow	0	-1	0

3.1.7 Growth analysis

A von Bertalanffy (VB) growth model was fit to the decimal age and length data for males and females separately, as well as to the combined data. The VB model has the form:

$$L_t = L_\infty(1 - e^{-k(t-t_0)})$$

where L_t is the fork length at age t, L_∞ is the mean asymptotic length, k is a relative growth rate parameter (year^{-1}), and t_0 is the age at which fish have a theoretical length of zero. We used maximum likelihood estimation assuming a Gaussian error structure with mean 0 and variance σ^2.

Akaike's information criterion (AIC) (Akaike 1974) was used to compare the sex-specific fits with the combined fit. Because no significant improvement was found by allowing for sex-specific growth parameters (see Results), a single VB growth model was fit to all of the data, including those fish for which sex was indeterminate. For comparison, a Richards growth model was also fit to all of the data. The Richards growth curve was parameterized as:

$$L_t = L_\infty(1 - 1/b * e^{-k(t-t_0)})^b$$

where all parameters are defined as for the VB model except the additional parameter b, which allows for more flexibility in the shape of the curve. Note that when $b=1$, the Richards equation is equivalent to the VB equation. We again used maximum likelihood estimation assuming a Gaussian error structure with mean 0 and variance σ^2.

To investigate whether there is spatial variation in growth, we modelled the length data using a generalized additive model (GAM) with age and latitude x longitude as 1- and 2-dimensional smooth terms respectively, and assuming a Gaussian distribution. We fit the model in R (R Core Team 2013) using the gam function in the mgcv library (Wood 2011), using the default smoothing method (penalized regression splines) and allowing the degree of smoothness for each term to be estimated automatically.

Based on the GAM results, we defined 4 areas corresponding roughly to the different spatial growth patterns observed, and fit separate VB models to the data within each of those areas.

Although we do not expect spatial variation in growth to correspond to the regions used for stock assessment (Fig. 1), for potential practical use in the assessment, we also fit separate VB models to the regions with at least 300 samples (region 3 and 4).

3.2 Reproduction and maturity

3.2.1 Study material

All ovaries collected between 2013 and 2016 (and available in Australia/New Caledonia) were selected from the WCPFC tissue bank for analysis. Only fish ≥ 80 cm FL were selected (n=157 cm FL) as this size is just below the minimum size at maturity in previous studies in the Pacific (e.g., Schaefer *et al.* 2005). An additional 85 ovary from fish >80 cm FL were obtained from the Chinese Taipei longline fishery to supplement the samples. Approximately half of ovaries selected from the tissue bank were subsampled at the landing port, placed in histological tissue cassettes, fixed in formalin and dehydrated in ethanol prior to shipment to Australia. The fish was not frozen prior to sampling, but were chilled rapidly in an ice slurry and then put on ice for the remainder of the fishing trip. For the remaining ovaries, the gonads were frozen and shipped to Australia. A cross-section was removed from the middle of one ovary lobe from each fish, while the ovary was frozen (not thawed), and fixed in 10% buffered formalin before being placed in a cassette. All gonad samples were embedded in paraffin and standard histological sections prepared (cut to 3 µm and stained with H&E). To increase the sample size, ovaries examined by Nicol et al (2011) (n=100) and sampled in 2010 and 2011 were included in the current work.

The majority of fish analysed were from regions 3 and 4 of the bigeye stock assessment and ranged between 81 and 178 cm FL (Fig. 2). Satellite-derived sea surface temperature (SST) data was obtained for each sampling location using CSIRO's spatial dynamics ocean data explorer (SDODE) (Hobday et al. 2006).
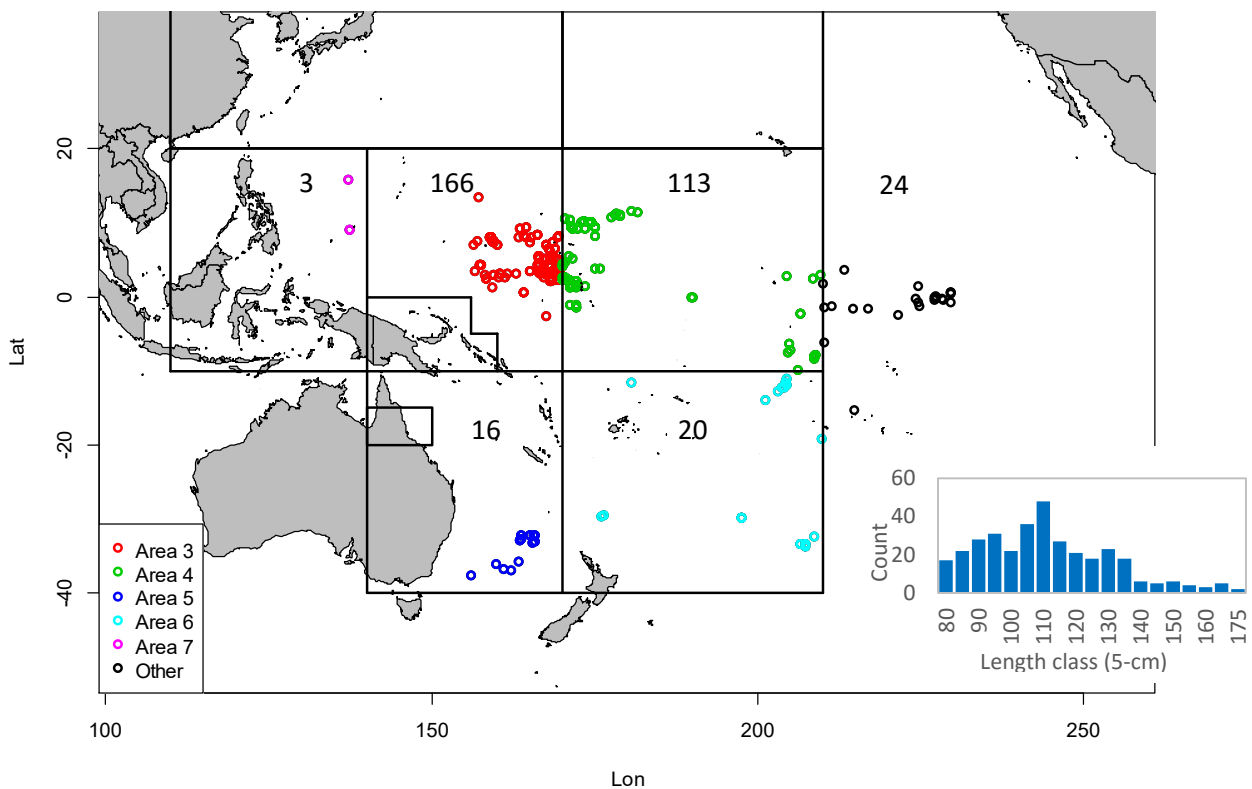
3.2.2 Histological classification

The histological sections were read to assess the ovarian development phase following Brown Peterson *et al.* (2011) and Farley *et al.* (2013). Females were classified into reproductive phases and sub-phases depending on the most advanced group of oocytes, post ovulatory follicles, atresia and maturity markers present in the ovary (Table 2; Appendix B).

The ovaries of immature fish were identified by the presence of unyolked oocytes as the most advanced present and no atresia of yolked oocytes or maturity markers. The ovaries of mature fish were identified by the presence of advance yolked oocyes, atresia of advance yolked oocyes and/or maturity markers. Mature females were subdivided into several phases. The spawning capable phase included (i) females with advance yolked oocytes but with no indication of spawning activity (non-spawning), and (ii) females with advance yolked oocytes and indications of spawning activity such as postovulatory follicles or migratory or hydrated oocytes (actively spawning). The regressing phase includes females with all yolked oocytes undergoing atresia indicating they have recently completed spawning for the season. The regenerating phase includes females that have also completed spawning, but have resorbed all the yolked oocytes in their ovaries so that the only indication of previous spawning activity are maturity markers in the ovary. The maturity markers considered useful for bigeye were thickness of the ovary wall, and/or the presence of brown bodies or residual hydrated oocytes.

Table 2. Number of females by histological classification. MAGO = most advanced group of oocytes, POF = postovulatory follicle. Maturity markers are the presence of brown bodies and/or residual hydrated oocytes.

MATURITY STATUS	PHASE	SUB-PHASE	MAGO AND POF STAGE	ATRESIA OF ADVANCED YOLKED OOCYTES	MATURITY MARKERS	COUNT
Immature	Immature		Unyolked, no POFs	Absent	Absent	127
Immature	Developing		Early yolked, no POFs	Absent	Absent	6
Mature	Spawning capable	Non-spawning	Advanced yolked, no POFs	α and β atresia may be present	Possible	25
Mature	Spawning capable	Actively spawning	Migratory nucleus or hydrated and/or POF's	α and β atresia may be present	Possible	92
Mature	Regressing		Unyolked or early yolked, no POFs	All yolked oocytes are in the α or β stages of atresia	Possible	39
Mature	Regenerating		Unyolked or early yolked, no POFs	Absent	Present	53
Total						342

3.2.3 Spawning frequency

Spawning frequency was estimated by the postovulatory follicle method of Hunter and Macewicz (1985a). This method uses the incidence of mature females with postovulatory follicles less than 24 hours old to define the fraction of the population spawning per day. Spawning frequency is inverse of spawning fraction.

3.2.4 Fitting maturity curves

The proportion of mature females at length or age was modelled using a logistic function:

Proportion mature = exp(alpha + beta*x) / {1 + exp(alpha + beta*x)} where x is either length (in cm) or age (in years).

We examined spatial variation in maturity at length using a GAM. Maturity state was treated as a binomial response variable with a logit link function, and modelled with fork length as a linear covariate (which equates to a logistic curve) and latitude x longitude as a 2-dimensional smooth term. We again fit the model in R (R Core Team 2013) using the gam function in the mgcv library (Wood 2011), using the default smoothing method and allowing the degree of smoothness for the spatial term to be estimated automatically.

We fit an analogous GAM to the maturity at age (instead of length) data, where age was estimated from length using the 4 area-specific VB growth curves derived in the growth analysis (see section 4.2.2 of the Results). Our preference would have been to use the direct age estimates from the otolith data, but only 101 fish with maturity data have a direct age estimate and they come from a narrow latitudinal range (Fig. 3), and thus are not sufficient for investigating spatial variation in maturity at age.
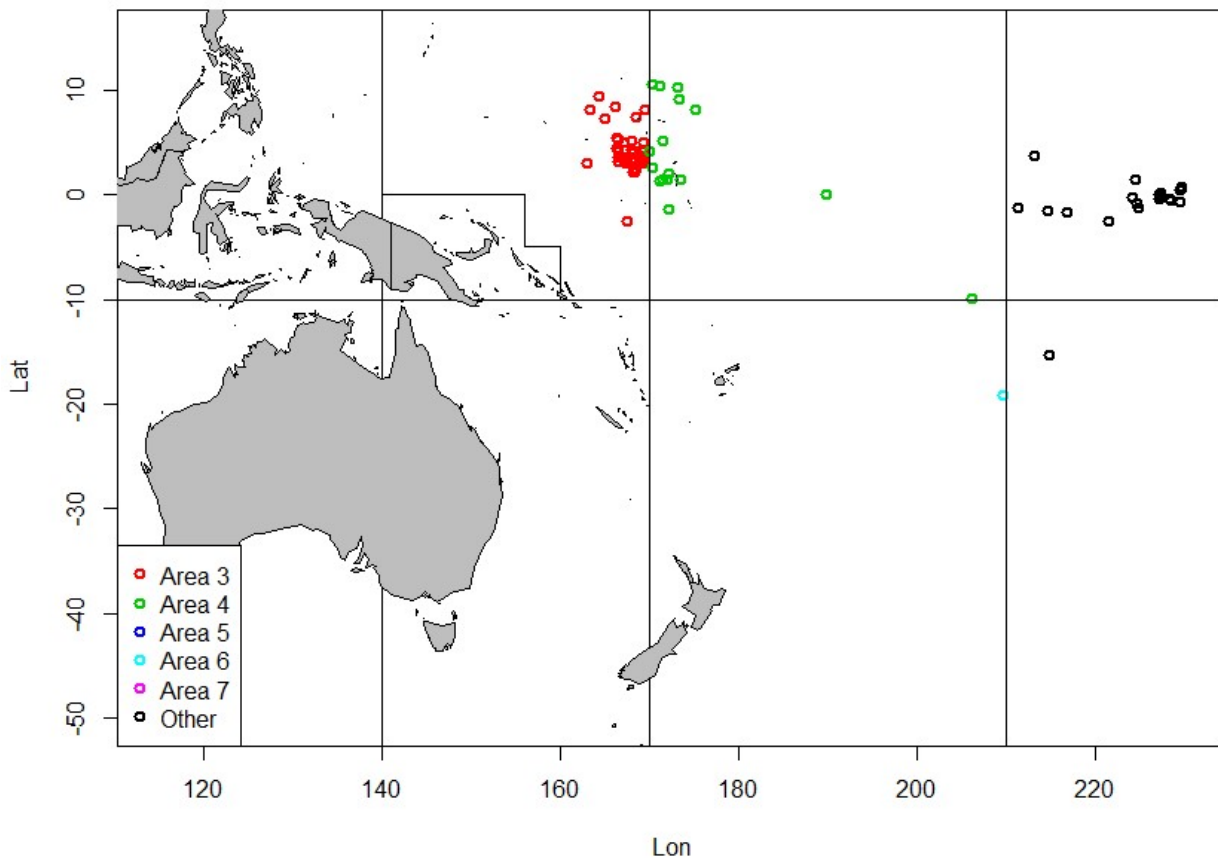
Figure 3. Map showing locations of maturity samples with direct (otolith) age estimates (n=101) by stock assessment region. Note that age data are only available for fish caught north of 25°S.

4 Results and discussion

4.1 Age estimation and validation

4.1.1 Annual age estimation and precision

Otolith weight was obtained for 653 of the 1053 samples; the remaining 400 samples were missing some part of the otolith. Otolith weight increased exponentially with fish size (Fig. 4). One clear outlier was removed from further analysis (45 cm FL and 0.080 g otolith weight). Counts of opaque growth zones were obtained for 1039 of the 1055 fish analysed. Counts ranged from 0-13 for females and 0-12 for males. The CV between readings by the primary reader was 7.55%, and between readings by the primary and secondary readers was 7.52%. No systematic bias was detected between readers (Fig. 5). Percent agreement in counts was 64.4%, and when counts differed, it was only by +/- 1 (Fig. 5).
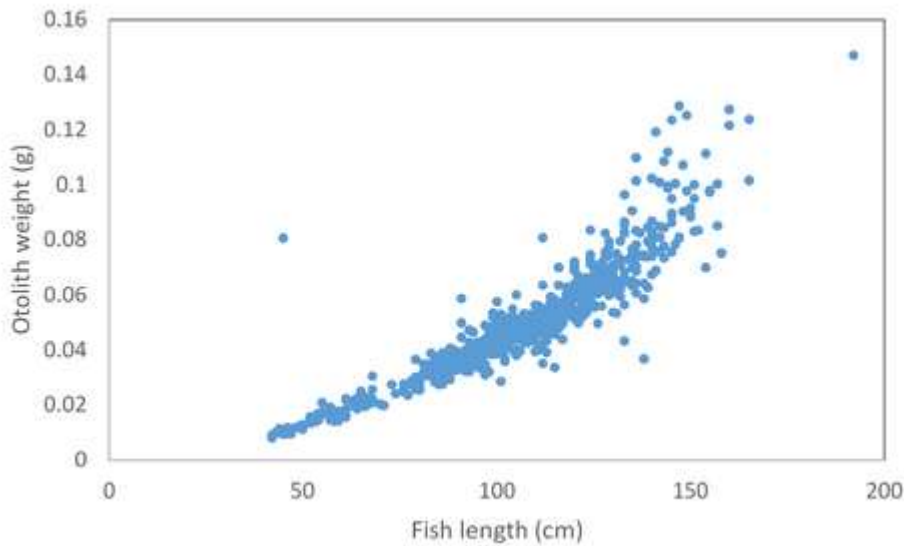
Figure 4. Relationship between fish length and otolith weight for bigeye selected for annual age estimation (n=653).
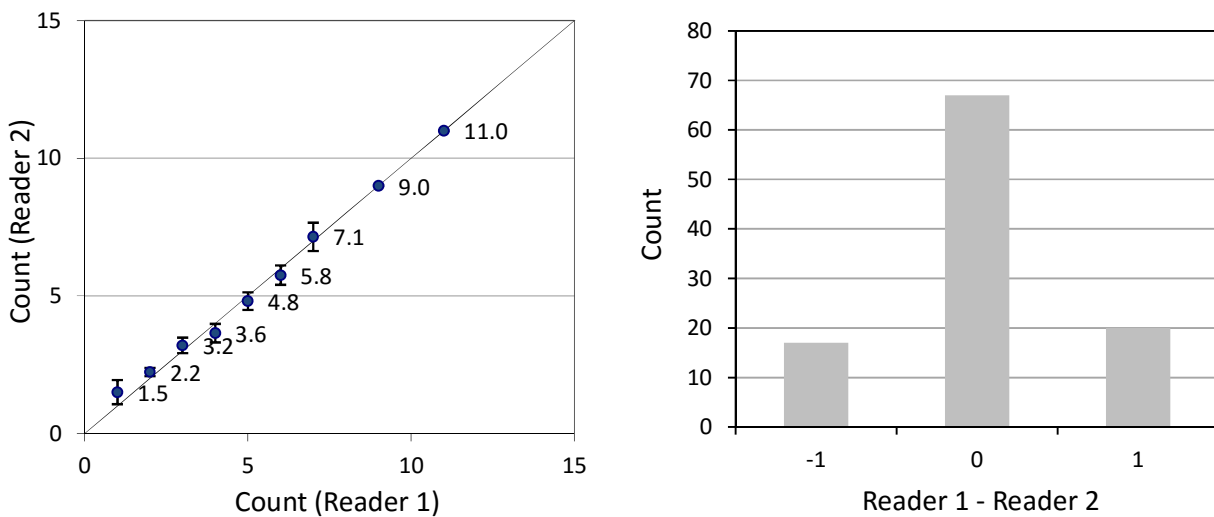

Figure 5. Age bias (left) and age difference (right) plots comparing final counts by two experienced readers.

4.1.2   Daily age estimation

Counts of microincrements were obtained for all 70 otoliths sectioned on the longitudinal plane. Age estimates ranged from 153 days (42 cm FL) to 781 days (111 cm FL). Longitudinally ground sagittae showed clear alternating opaque and translucent zones along much of the long arm (Appendix C). The zones were more uniform along a transect that ran approximately half way between the sulcal and distal edge. The first 30 or so zones were relatively wide with subsequent zones slowly reducing in width until at a count of approximately 100 zones they became reasonably consistent in width and pattern. No obvious transition point in zone structure or annual check was observed, however, the interpretation of microincrements past a count of 300 was more difficult due to the presence of split zones and multiple zones that converged into each

other. While microincrements were counted past 300, and in many samples the zone pattern was still clear in outer areas of the otolith, we were far less confident in the total zone count representing the true age of samples greater than 300 days.

Microincrement count increased linearly with increasing fish size (Fig. 6). When compared directly to the annual counts from the same sample (fish), the 1:1 line of agreement diverged at approximately 1.2 years with microincement counts underestimating age compared to annual counts (Fig. 7). Back-calculated hatch dates from the daily age estimates ranged throughout the year suggesting that for these samples, hatching occurred over 12 months. When limited to those samples less than 300 days, the back calculated hatch dates range from April to December.
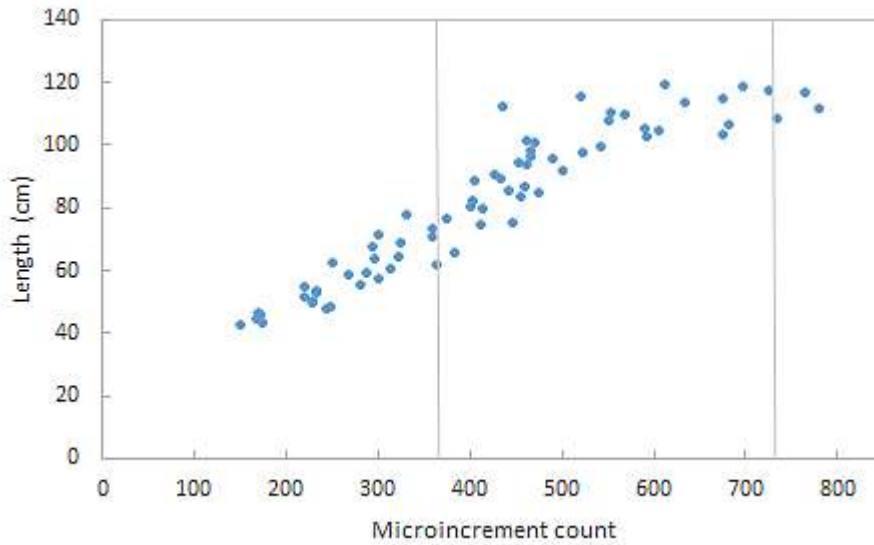

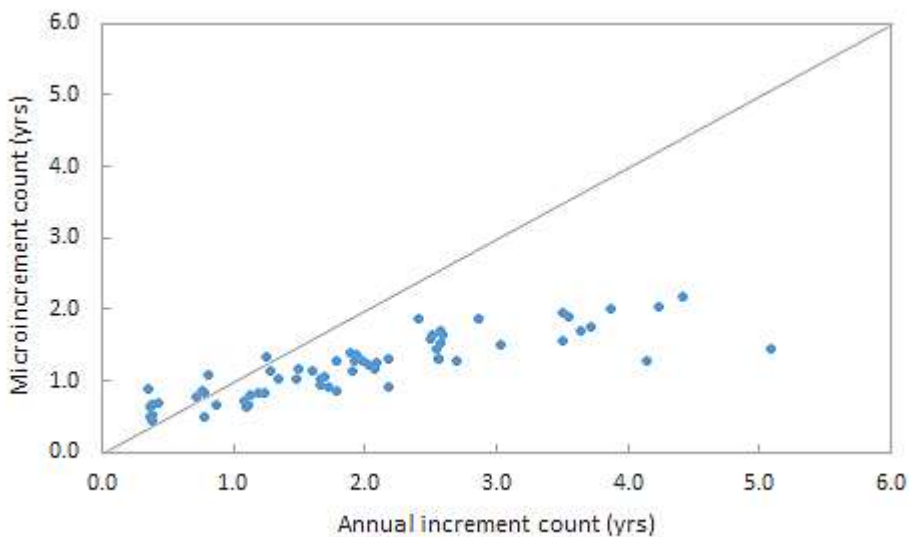**Fig. 6. Relationship between fish length (cm) and daily counts from longitudinal sectioned otoliths.**

Fig. 7. Comparison of daily and annual counts from sectioned otoliths sampled from the same fish.

Counts of microincrements were obtained for all 30 otoliths prepared on the transverse plane. Age estimates ranged for 224 days (56 cm FL) to 857 days (118 cm FL). Again, the zone structure was very clear initially. The first 30 zones were far wider than subsequent zones, with zones gradually reducing in width out to approximately 80–100 increments where the zone pattern became regular (Appendix D).

In most of the otoliths examined, at a count of approximately 150 and 180, a transition area in the otolith morphology was observed. This transition point was characterised by a relatively diffuse area where the zones change in pattern and optical clarity (see Appendix D). The zones subsequent to the transition point were difficult to interpret and included areas with split zones and converging zones. The pattern of zone deposition was far less concentric than the zones prior to the transition point. As with the longitudinally prepared samples, we were only confident of the assignment of an age past a certain point. In transverse sections, this was at a microincrement count of approximately 180.

In both preparation methods, it is suggested that the area that represents the point where ageing becomes uncertain is related to the formation of the first major discontinuous zone. Morales-Nin (1988) indicated that in a study of tropical fish, daily zones were not likely to be deposited (or at least not able to be detected by either light or scanning electron techniques) at a daily rate throughout this zone and that counting microincrements through the opaque zone would lead to an underestimation of age. In our case, the difference in the counts is likely to be due to the characteristics of the sectioning plane and the relative otolith growth. The otoliths prepared longitudinally are sectioned on the primordium to post rostral axis and when compared to the transverse axis there is far more otolith material. Therefore, the discontinuous check or transition area may not be as sudden when compared to the check observed on the transverse preparations and allow for more microincrements being observed under light microscopy.

Our results are consistent with Williams *et al.* (2013) where, for bigeye, the divergence from the 1:1 line of agreement (daily vs annual age) began slightly later than the first year in longitudinal sections and less than 1 year in transverse sections.

4.1.3 Indirect (annual) age validation

The annual periodicity of the 2nd to 9th opaque zone in sectioned otoliths has been directly validated for bigeye in the southwest Pacific Ocean (Clear *et al.* 2000; Farley *et al.* 2006). Additional indirect validation was undertaken by Farley *et al.* (2006) to confirm the location of the 1st two opaque zone using counted of microincrements in otoliths sectioned on the transverse plane.

In the current study, the distance from the first inflection point to the 365th microincrement was available for 20 otoliths (mean 1122 µm ± 16.1 SD) sectioned on the transverse plane. This measurements are consistent with Farley *et al.* (2006) (1124 µm). A comparison of this measurement with the distance to the first two opaque zones in annually age otoliths further confirm that the first annual opaque zones are being successfully identified in transverse sectioned otoliths (Fig. 8). The mean distance from the first inflection point to the first opaque zone in annually aged otoliths was 994 µm (± 97 SD), which is consistent with the general area where, in daily transverse sections, the zone interpretation became difficult.
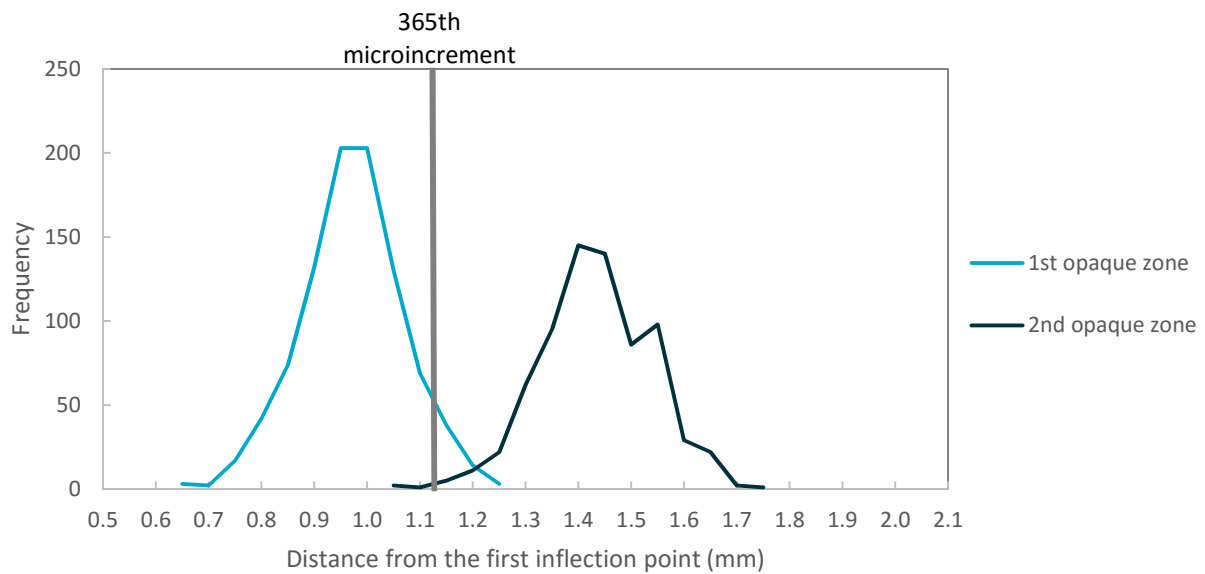
Figure 8. Histograms of the distance from the inflection point in transverse sectioned otoliths to the first two opaque zones on otoliths measured for annual age estimation. The mean distance to the 365th increment (age 1) from microincrement counts is indicated.

Marginal increment analysis is only suitable for young fish (Campana 2001) so we carried it out for ages 2-3 years only. For otoliths collected north of 10°S, there appears to be a seasonal cycle in mean MIR with the highest values in ~December to March and the lowest value in ~June to August, although April had the lowest mean MIR value and October had the highest MIR value (Fig. 9). This slightly inconclusive result may be due to bias from samples collected over a too long a period (4 years), insufficient sample sizes by age class (e.g., possibly for April), and difficulty in accurately measuring increment positions. The annual pattern in MIR was not clear for otoliths collected south of 10°S due to low sample sizes (Fig. 9).

The edge type analysis suggests that opaque zones form between April and September in otoliths samples north of 10°S, as the proportion with narrow and intermediate edges was highest (Fig. 10). This pattern seems clearer for otoliths samples south of 10°S, where the proportion of otoliths with narrow and intermediate edges peaked in July.

Marginal increment and edge type analysis are both difficult to carry out due to small samples sizes and the difficulties of measuring increments accurately (Campana 2001). However, based on the current work, we suggest that opaque zones in the otoliths examined formed between April and September.
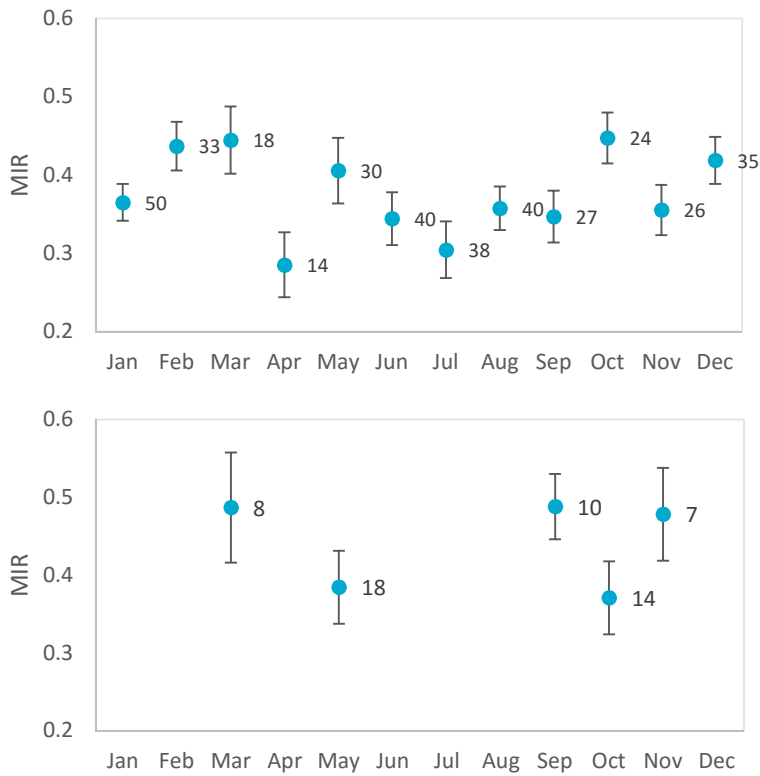
Figure 9. Mean (+/- SE) monthly marginal increment ratio (MIR) for bigeye tuna otoliths sampled north (top) and south (bottom) of 10°S. Sample size is shown next to the mean; only months where n ≥ 5 are shown. MIR data were restricted to age 2 and 3.
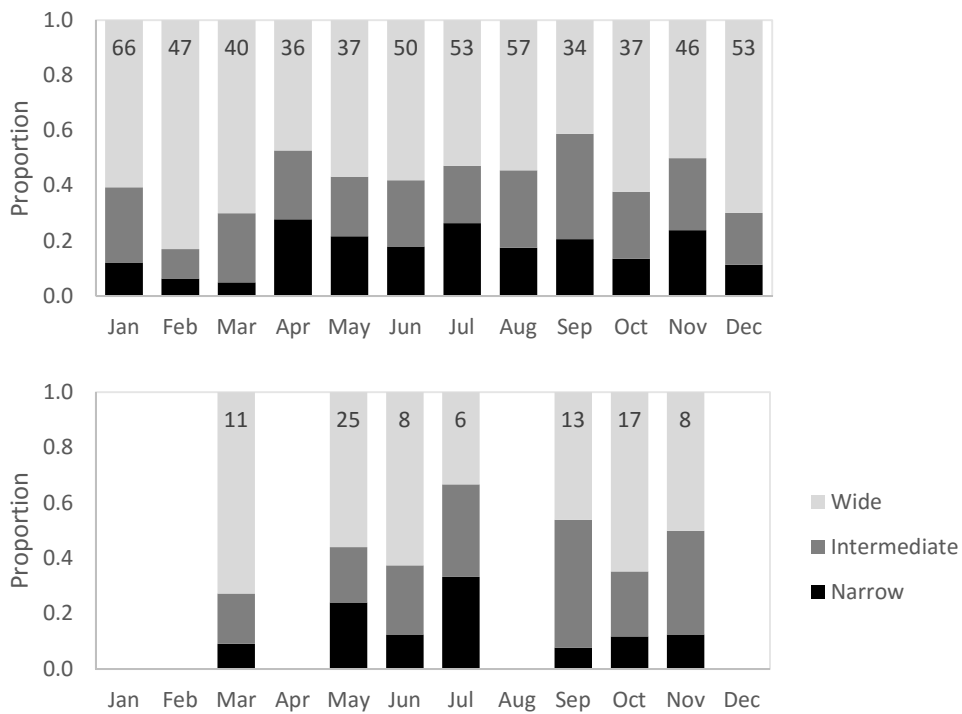
4.1.4 Decimal age

Annual age estimates ranged from 0.25 to 13.67 years and there was substantial variation in length-at-age (Fig. 11; Appendix E). We found that annual age (and the VB growth curve; see section 4.2.1 below) was consistent with the daily age estimates up to age 1 (Fig. 11). After that age, microincrement counts appear to underestimate annual age. This is not unexpected since the transition point mentioned in section 4.1.2, where microincrements became difficult to interpret, is likely to correspond to the first annual discontinuous (opaque) zone. The variability observed in length at (annual) age for the youngest ages is also not unexpected since annual age estimates relies on setting a single birthdate and zone formation date. For 0+ samples, decimal age is just a reflection of an estimated single birthdate and the time of capture whereas for the microincrement counts (at least out to 300) should be able to accurately estimate their actual age. The important point was that the age algorithm used did not result in any of these 0+ samples being assigned a negative age, and the daily ages and VB growth curves are consistent in the first year. These results suggest that the algorithm used to convert annual zone counts to decimal ages daily is reasonable.
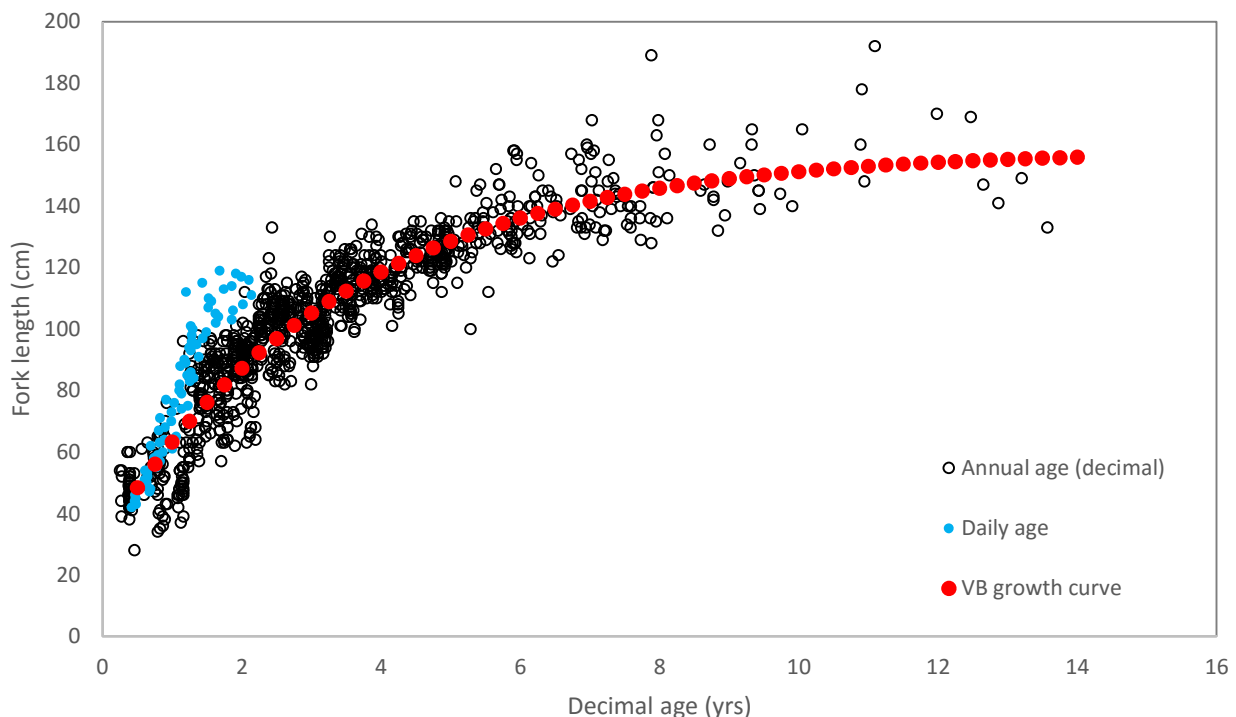

Figure 11. Estimated length at age from counts of annual increments (annual age) and counts of microincrements (daily age). The von Bertalanffy (VB) growth curve is also shown (see Table 6 below; VB for all fish).

16

4.2 Growth analysis

4.2.1 Model selection and growth curves for regions 3 and 4

Of the 1039 fish with a decimal age assigned, 616 were males, 272 were females and 151 had an indeterminate or unspecified sex. The parameter estimates and mean growth curves for males and females are similar (Fig. 12; Table 3), and the AIC values suggest there is no significant improvement in the model fit by allowing for sex-specific parameters (the AIC for males plus AIC for females is 6501.6, which is 0.6 units more than the AIC for the combined data; Table 3).

The mean growth curve estimated from the Richards model is almost identical to the mean growth curve from the VB model (Fig. 13), and the AIC values indicate that the Richards model does not provide a statistically better fit (Table 3).

The results from fitting a VB model to the data from regions 3 and 4 (greatest sample size) suggest that growth does not vary substantively between these areas (Fig. 14; Table 4). This is not surprising since most samples (86%) were obtained from a restricted area between 160 and 180°E, which straddles the border separating the two regions.

The results from fitting a VB model to the data from regions 3-8 combined are in Fig. 15 and Table 4. McKechnie et al. (2017) compared this growth curve with that estimated from tagging data and found no significant effect on estimates of parameters such as L_∞.

Table 3. Parameter estimates from fitting a von Bertalanffy (VB) growth model to the bigeye age and length data for males (M), females (F), and males and females combined (M+F), as well as from fitting a VB model and a Richards model to all of the data (All), which includes fish with indeterminate sex. Standard errors for the parameter estimates are given in parentheses. The sample size (n) and AIC value for each model are also presented.

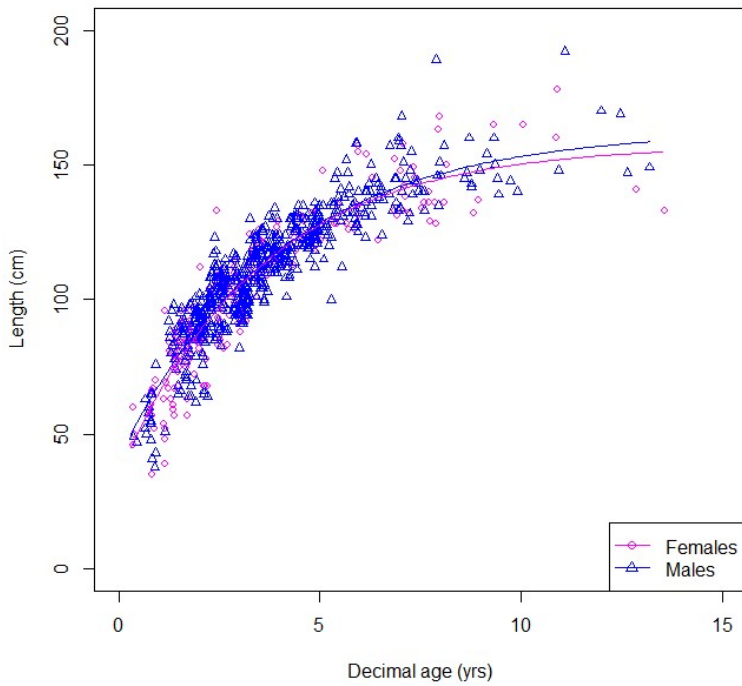| MODEL	DATA	n	L_∞	k	t_0	b	σ	AIC
VB	M	616	162.9 (3.0)	0.251 (0.016)	-1.15 (0.13)	-	9.1 (0.26)	4473.46
VB	F	272	157.5 (3.6)	0.284 (0.023)	-0.89 (0.14)	-	9.9 (0.43)	2028.15
VB	M+F	888	160.3 (2.2)	0.268 (0.013)	-1.01 (0.09)	-	9.4 (0.22)	6501.01
VB	All	1039	158.1 (1.8)	0.292 (0.011)	-0.75 (0.05)	-	9.7 (0.21)	7669.54
Richards	All	1039	159.0 (2.9)	0.282 (0.030)	-0.89 (0.41)	0.94 (0.16)	9.7 (0.21)	7671.42

Figure 12. VB growth model fit to male and female data separately. There is no significant difference between sexes based on AIC.
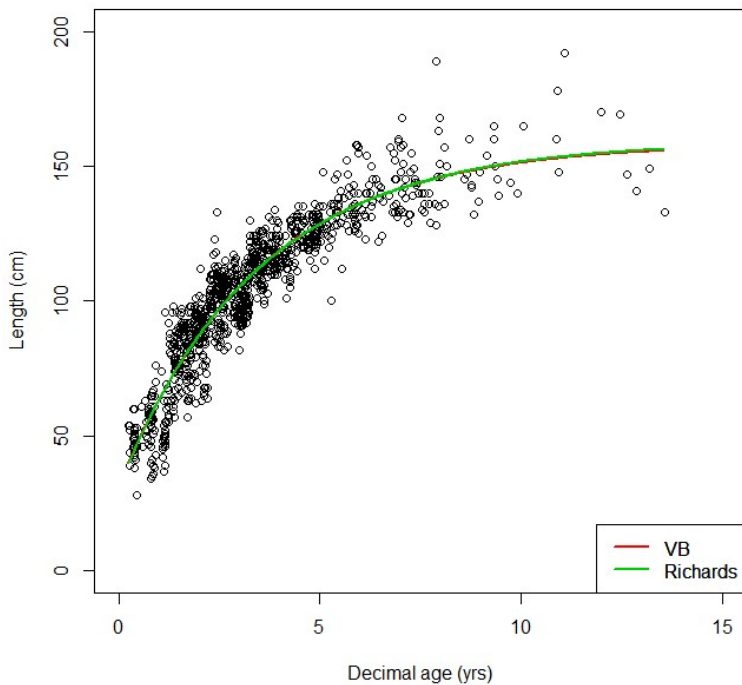
Figure 13. Comparison of the mean growth curves estimated from the von Bertalanffy (VB) and Richards growth models fit to all of the age and length data (black circles). The VB model is preferred based on AIC since it involves one less parameter.

Figure 14. VB growth models fit to the data from regions 3 and 4 of the bigeye stock assessment (see Fig. 1).

Figure 15. VB growth model fit to the data from the stock assessment regions only (regions 3-8).

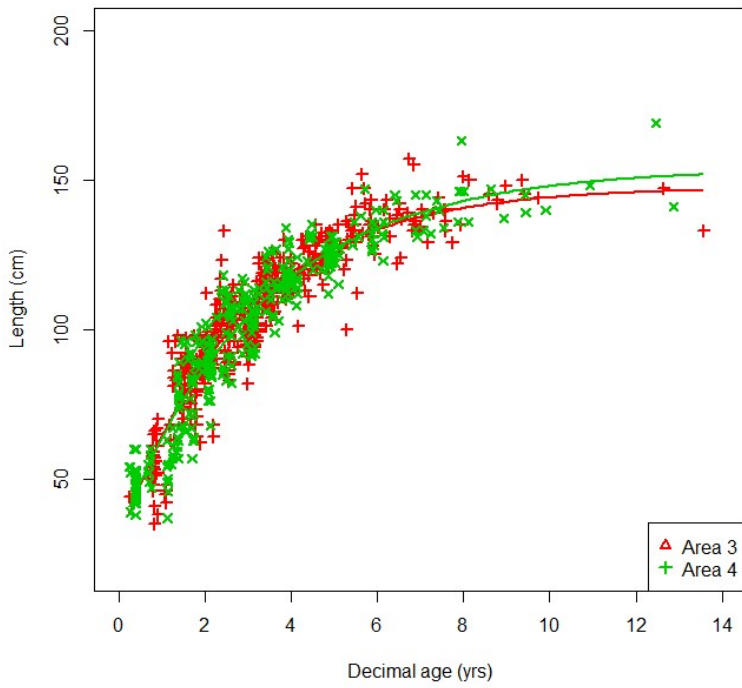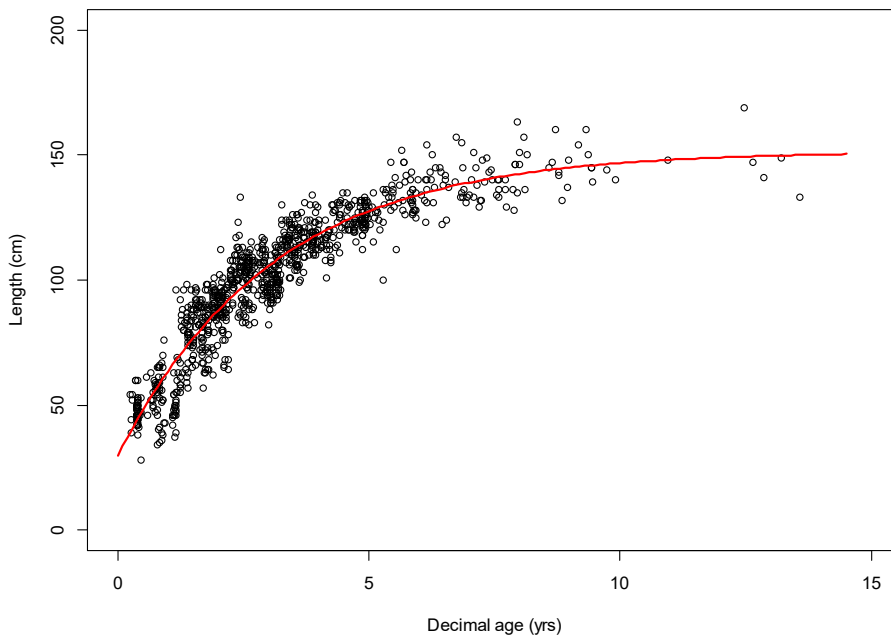**Table 4. Parameter estimates from fitting a von Bertalanffy (VB) growth model to the bigeye age and length data within stock assessment areas 3 and 4, and areas 3 to 8 combined (see Fig. 1). Standard errors for the parameter estimates are given in parentheses. The sample size (n) and size range of fish within each area is also given.**

Area	n	FL range (cm)	Mean FL (cm)	L_∞	k	t_0	σ
3	491	35-157	104.0	147.5 (2.3)	0.36 (0.02)	-0.61 (0.09)	8.9 (0.3)
4	330	37-169	97.0	153.8 (2.8)	0.30 (0.02)	-0.77 (0.07)	8.8 (0.3)
3-8	987	28-169	100.1	151.4 (1.8)	0.33 (0.01)	-0.67 (0.05)	9.2 (0.2)

4.2.2   GAMs to investigate spatial effects

The summary results from fitting a GAM to length with age and latitude x longitude as smooth terms are given in Table 5. Both smooth terms are significant, suggesting that growth does vary spatially. Plots of the estimated predicted lengths from the GAM are shown in Fig. 16; the top panel shows predicted lengths at age when latitude and longitude are fixed at the mean values in the dataset (1.04°N, 173.6°E), and the bottom panel shows spatial predictions of length when age is fixed at the mean value in the dataset (3.3 yrs). Although fitting age as a smooth term using the default degrees of freedom (8.5) results in a more "wavy" curve than a VB model, constraining the degrees of freedom to be smaller such that the curve more closely resembles VB growth has very little effect on the pattern of the spatial smooth. Generally speaking, the spatial smooth suggests that length at age is greater (yellow) at the westernmost (<140°E) and easternmost (>205°E) longitudes, and lower (red) within the central longitudes (140-205°E). Within the central longitudes, there also appears to be some differences with latitude, with length at age being greatest above ~5°S. This spatial pattern holds true when age is fixed at different values (by necessity since the model was not fit with an interaction between age and space).

Based on these results, we defined 4 new areas (A, B, C, D) roughly corresponding to regions of similar growth (Fig. 17), and fit VB curves to the age and length data within each (Table 6, Fig. 18). We caution, however, that the data are limited in terms of spatial distribution and age/length coverage within spatial regions for fully evaluating differences in growth. For example, very few small fish (<80 cm FL) were aged from areas A and B, and (consequently) the VB growth curved indicated greater length at age for fish up to age ~3 compared to the other two areas (Fig. 18). Area C had the largest number of age estimates from small fish (<80 cm) and area D had the largest number of age estimates from large fish (>150 cm FL) fish.

Based on the growth curves obtained, however, bigeye appear to growth faster in Area D than Areas A-C. This is consistent with faster growth rates obtained for bigeye in the EPO from analysis of otoliths and tag-recapture data by Aires-de-Silva (2015). The two largest fish sampled (189 and 192 cm FL) in area D were aged as 7.8 and 11.1 years respectively (Appendix E.2, E.3). So although these were large fish, they were not the oldest obtained in the study.

Table 5. Summary output from fitting a GAM to length with age and latitude x longitude as smooth terms (produced by the summary.gam function in R).

```
Family: gaussian
Link function: identity

Formula:
Length ~ s(Decimal_age) + s(Lon, Lat)

Parametric coefficients:
           Estimate Std. Error t value Pr(>|t|)
(Intercept) 102.0924     0.2611     391   <2e-16 ***
---
Signif. codes:  0 '***' 0.001 '**' 0.01 '*' 0.05 '.' 0.1 ' ' 1

Approximate significance of smooth terms:
                 edf Ref.df      F p-value
s(Decimal_age)  8.445  8.906 490.70  <2e-16 ***
s(Lon,Lat)     21.132 25.510  10.86  <2e-16 ***
---
Signif. codes:  0 '***' 0.001 '**' 0.01 '*' 0.05 '.' 0.1 ' ' 1

R-sq.(adj) =  0.913   Deviance explained = 91.6%
GCV = 72.979  Scale est. = 70.832     n = 1039
```
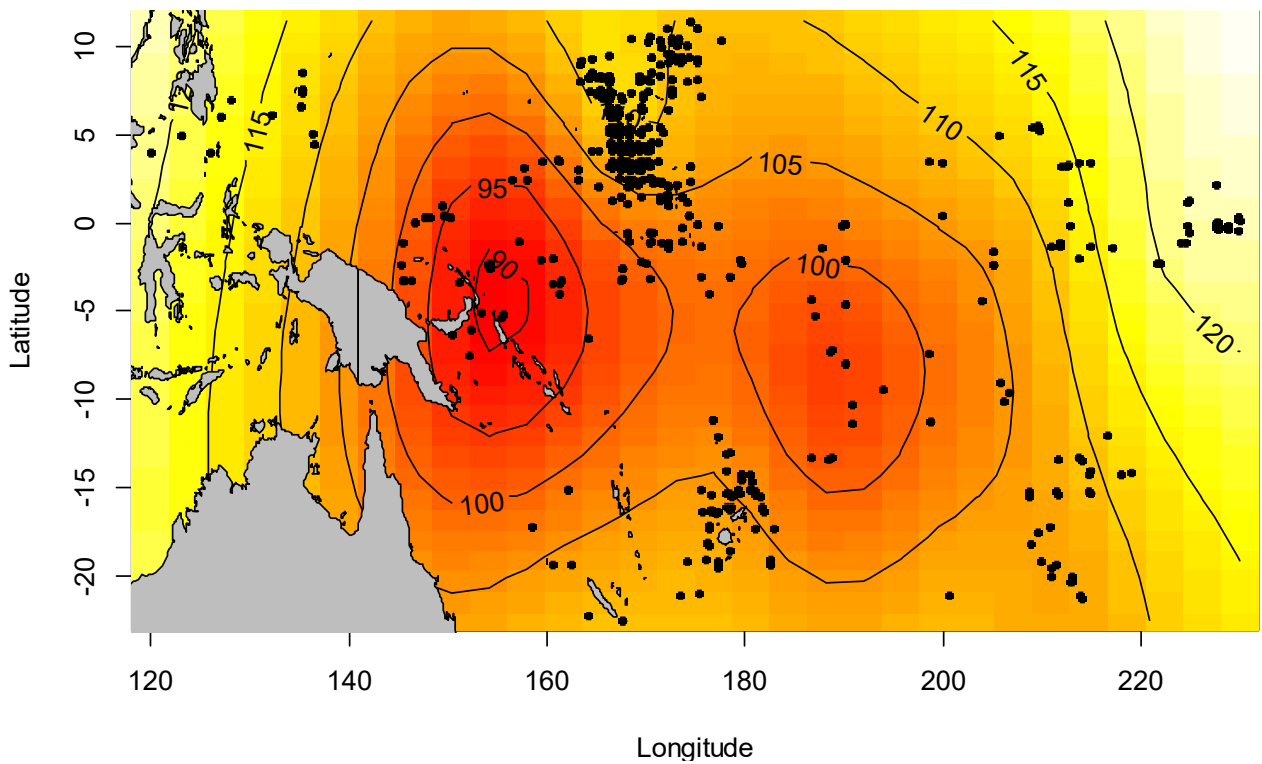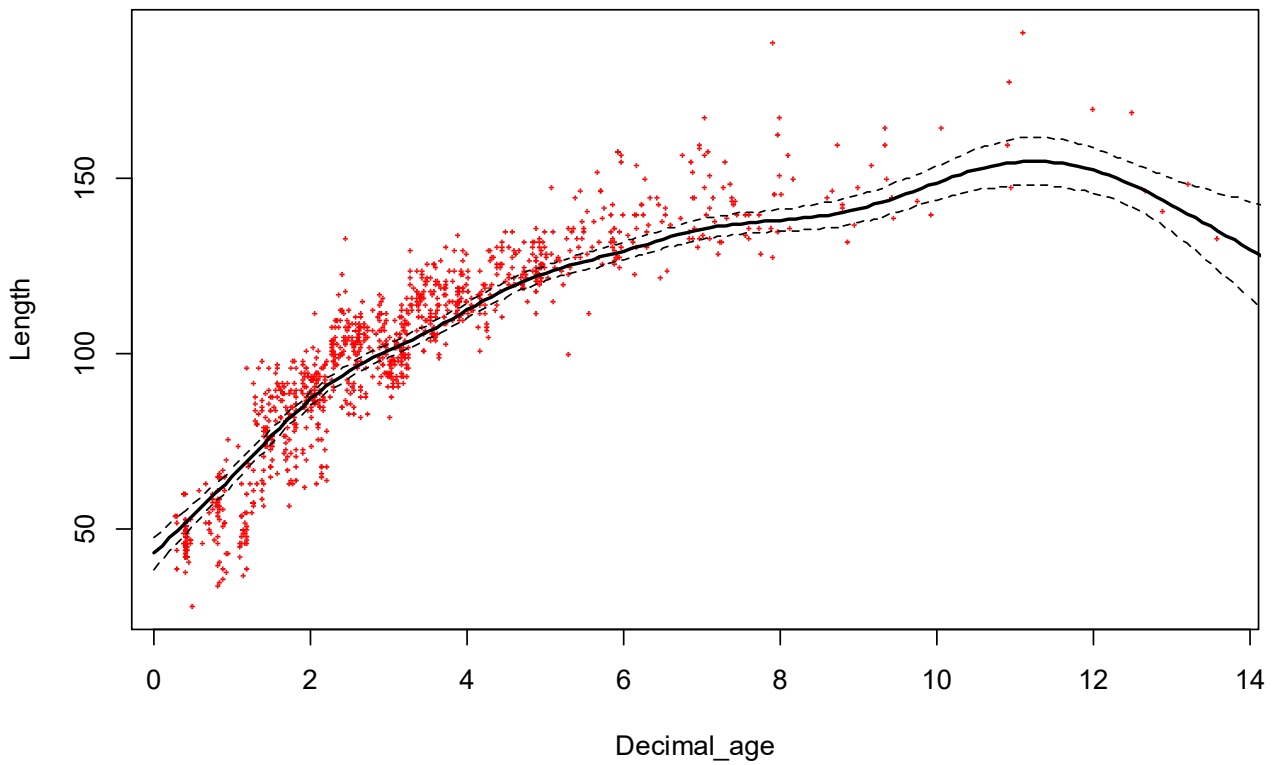
Figure 16. Results from fitting a GAM to length with age as a smooth term (top) and longitude x latitude as a 2-dimensional smooth term (bottom). In the top panel, predicted lengths at age were calculated at the mean latitude (1.04°N) and longitude (173.6°E) in the dataset; in the bottom panel, predicted lengths at each spatial coordinate were calculated at the mean age (3.3 ys) in the dataset.
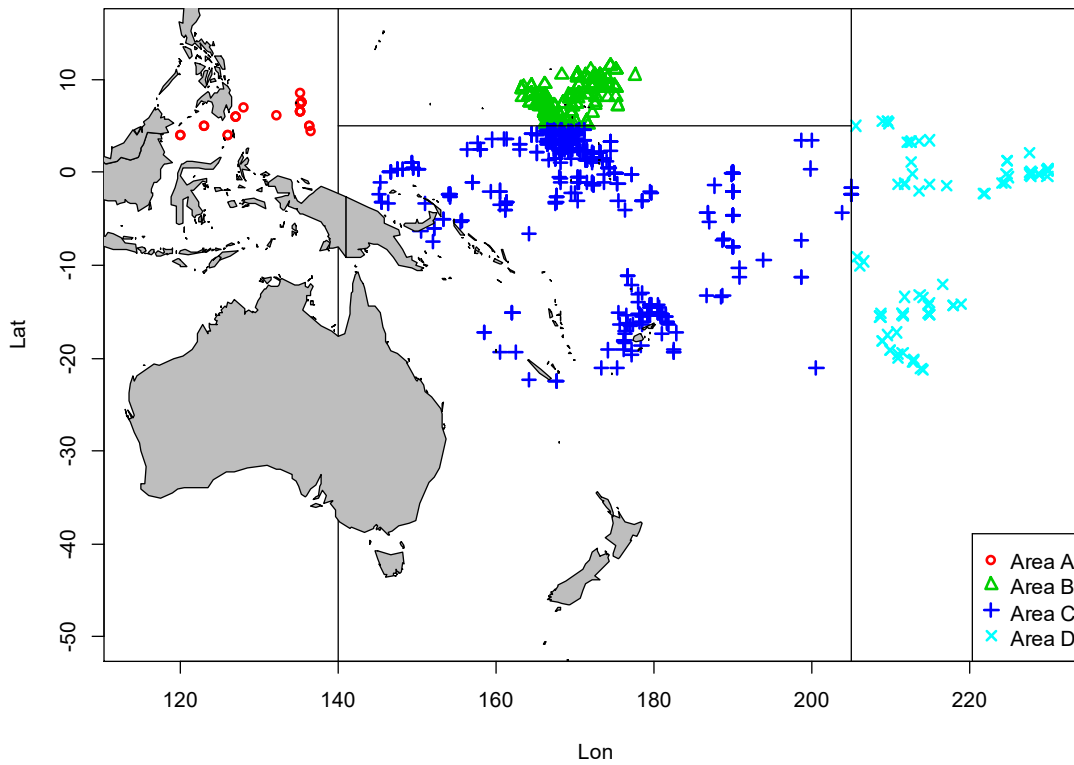
Figure 17. Map showing newly defined areas corresponding approximately to the different spatial growth patterns observed in the GAM results (see Fig. 16).

Table 6. Parameter estimates from fitting a von Bertalanffy (VB) growth model to the bigeye age and length data within the 4 spatial areas defined in Fig. 17. Standard errors for the parameter estimates are given in parentheses. The sample size (n) and size range of fish within each area is also given.

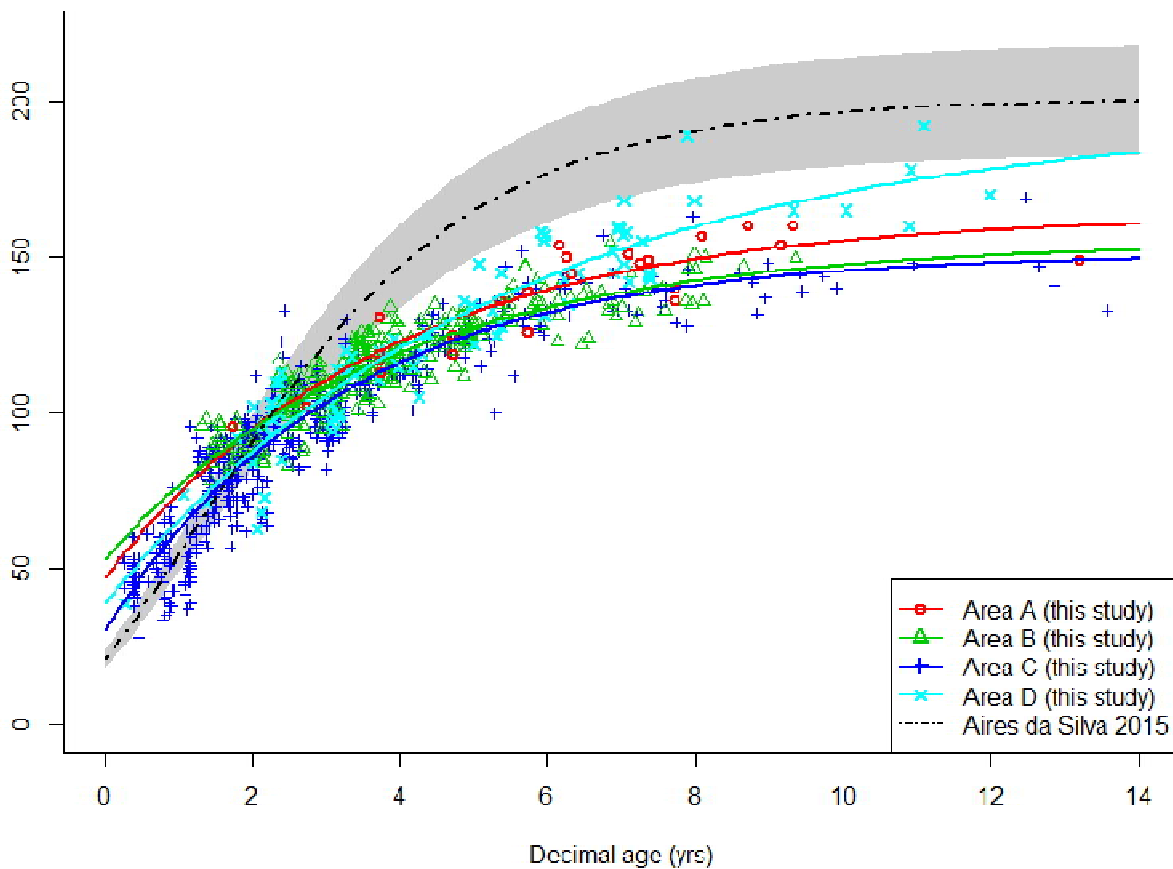| AREA	n	FL range (cm)	Mean FL (cm)	L_∞	k	t_0	σ
A	24	96-160	136.5	163.5 (7.1)	0.26 (0.06)	-1.3 (0.8)	7.5 (1.1)
B	299	78-155	115.9	154.8 (4.1)	0.26 (0.03)	-1.6 (0.3)	6.7 (0.3)
C	633	28-169	91.5	151.0 (2.4)	0.31 (0.01)	-0.7 (0.1)	9.7 (0.3)
D	83	39-192	123.5	194.9 (10.8)	0.19 (0.03)	-1.2 (0.4)	10.4 (0.8)

Figure 18. VB growth models fit to the data from each of the 4 spatial areas defined in Fig. 17. The integrated growth curve (and variability) estimated by Aires-da-Silva et al. (2015) for the eastern Pacific Ocean is also shown.

4.3 Reproduction and maturity

4.3.1 Ovary material

A large proportion of the ovaries examined in this study were frozen before being subsampled, fixed and histologically examined. Although freezing can affect the quality of the histology, it did not affect our ability to correctly identify histological features including late stages or atresia/maturity markers and postovulatory follicles. Degradation of the ovary was reduced by subsampling the ovary while it was frozen, rather than thawed. Frozen ovary material has been used successfully in several recent reproductive studies on tunas, swordfish and wahoo (e.g., Farley et al. 2013; 2014; 2015; 2016; Zischke et al. 2013). As noted in Farley et al. (2016), maturity markers are particularly obvious/clear in ovary histology that has been prepared from material frozen prior to fixation. However, it is recommended that experienced readers are used to assess frozen-fixed histological material.

4.3.2   Spawning area and season

Of the 343 ovaries examined, 133 were classed as immature, 117 as spawning capable and 92 as regressing/regenerating (Table 2). Given the spatial distribution of samples and reproductive phase of females, we divided the study region into two regions: north and south of 20°S. In the south, only immature (n=16) and regressing/regenerating (n=12) females were present (Fig. 19). The SST at the sampling locations ranged from 17.8 to 20.0°C.

In the north, females in all reproductive phases were present (117 immature, 117 spawning capable and 81 regressing/regenerating). Spawning capable females occurred between 12°N and 12°S and 137°E and 130°W (137-230°E in Fig 19). They were present throughout the year but in slightly higher relative abundance in May and August-October, although sample sizes were too low to conclusively define a spawning season (Fig. 19; 20). Sun *et al.* (2013) and Schaefer et al. (2005) found that bigeye spawn throughout the year in the northwest and eastern Pacific, respectively. However, Sun et al (2006; Fig. 4) showed that spawning peaked in June and July in the northwest Pacific.

Spawning capable females were present in SSTs between 27.7 and 30.3°C, but the percentage of actively spawning and non-spawning females was highest at SSTs between 28 and 29°C (Fig. 21). Conversely, the percentage of females classed as immature or post-spawning (regressing/regenerating) were highest at SSTs between 29 and 30°C. The large number regressing or regenerating females in this region (n=81) confirms that not all females are reproductively active in waters >24C in the western Pacific.
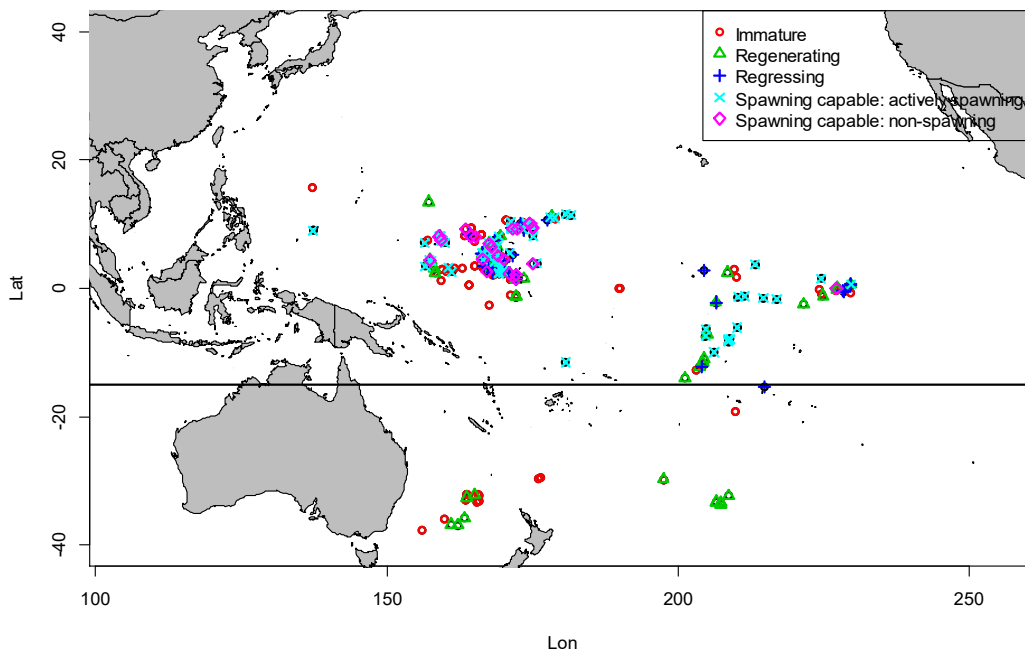

Figure 19. Map of the ovary sampling locations. Different colours and symbols represent different reproductive phases.
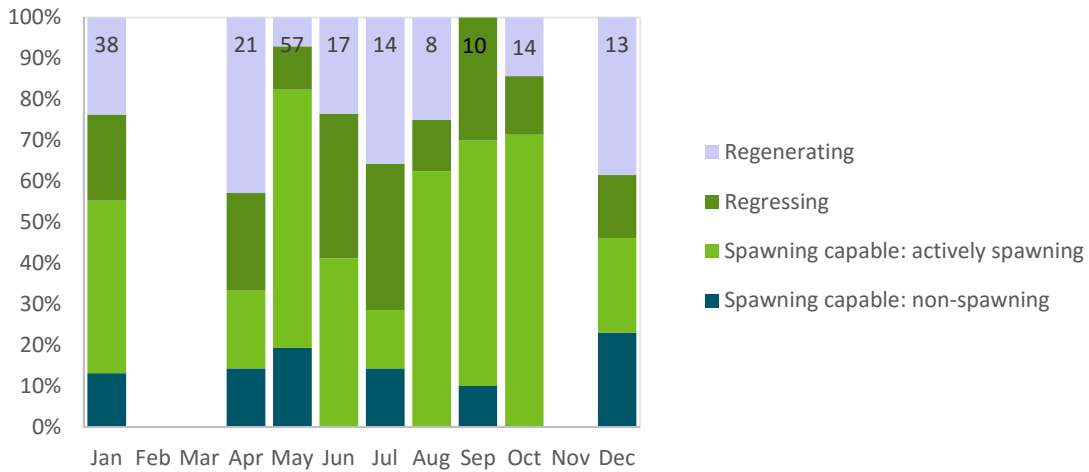
Figure 20. Percent of mature females by reproductive phase and month in the area north of 15°S (if n>5). Sample sizes shown at the top of the bars.
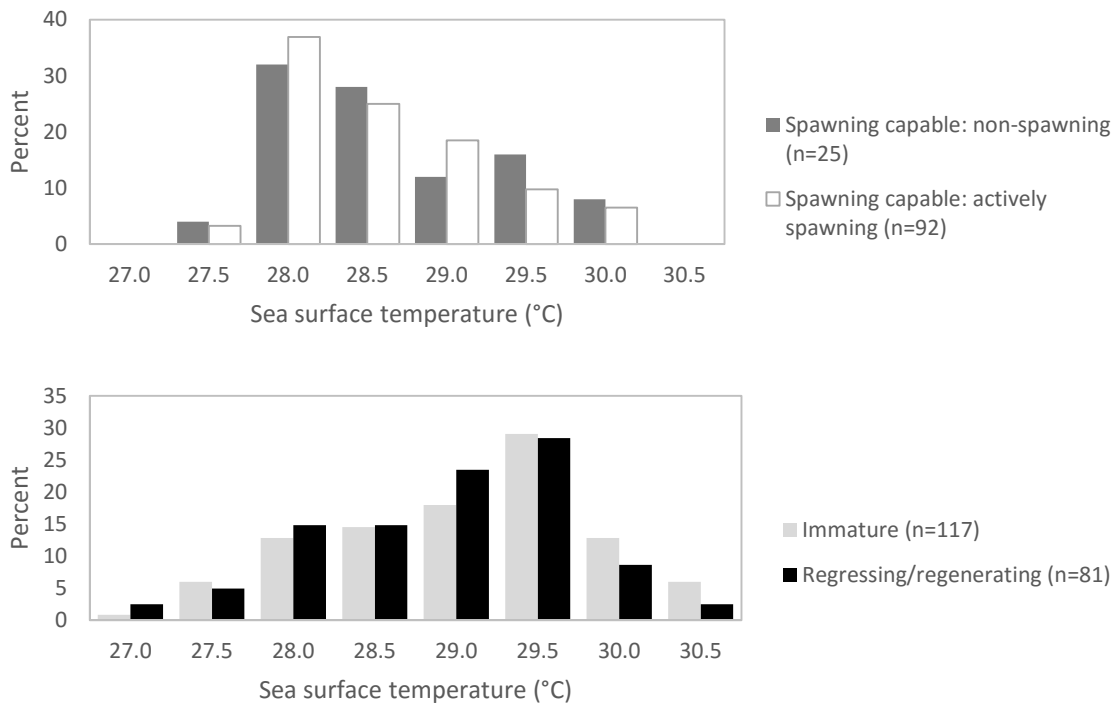

Figure 21. Percent of mature females by reproductive phase and month in the area north of 20°S.

4.3.3   Spawning frequency

The fraction of bigeye spawning was 0.33, suggesting that the mean spawning frequency (time between successive spawnings) was 3.03 days (Table 7). However, when the data were restricted to spawning capable females, the mean spawning interval was 1.36 days. However, when actively spawning, bigeye are capable of spawning almost daily (spawning interval of 1.08 days; Table 7).

A trend in spawning frequency by fish size was found when the data were pooled into 10-cm length classes to obtain adequate sample sizes (Fig 22). Mean spawning frequency was relatively long for small fish (13 and 6 days for fish in the 90 and 100 cm length classes, respectively) and relatively short for larger fish (1.6 to 3.0 days for length classes ≥110 cm) (Fig. 22).

Table 7. Estimated spawning fraction and spawning frequency of females by maturity status/phase. Analysis was restricted to the spawning altitudes (15°N-15°S).

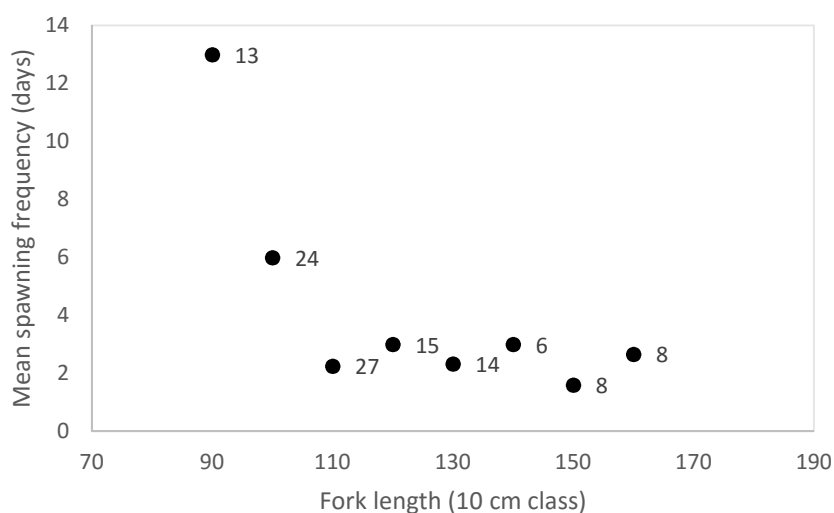| MATURITY STATUS/PHASE	NO. WITH POST OVULATORY FOLLICLES	NO. MATURE	FRACTION SPAWNING PER DAY	MEAN SPAWNING INTERVAL
All mature	39	118	0.33	3.03
Spawning capable (all)	39	53	0.74	1.36
Spawning capable - actively spawning	39	42	0.93	1.08

Figure 22. Mean spawning frequency of bigeye by 10-cm length class caught. Analysis was restricted to the spawning latitudes (15°N-15°S). Sample sizes are indicated.

4.3.4   Maturity at length/age for regions 3 and 4

Females classed as immature ranged in length from 81 to 136 cm FL while mature females ranged from 87 to 178 cm FL. Estimates of length and age at 50% maturity (L_{50} and A_{50}) for regions 3 and 4 combined were 103.0 cm and 2.85 years respectively (Table 8). Based on our samples, estimates of L_{50} and A_{50} differed slightly between these regions suggesting that spatial variation in maturity may exist (Table 8; Fig. 23) (also see next section). The L_{50} estimates obtained are similar to those of Sun et al. (2013), Zhu et al. (2010) and Farley ey al. (2006) for bigeye in the western Pacific, but lower than obtained by Schaefer et al. (2005) in the eastern Pacific (Table 8).

Table 8. Estimated length and age at 50% maturity (L_{50} and A_{50}) values in the current study for regions 3 and 4 of the bigeye stock assessment. Estimates of L_{50} and A_{50} are also shown from other studies of female bigeye tuna in the Pacific Ocean (PO).

| Study	Method	Location	n	L_{50} (cm)	A_{50} (yrs)
Current study	Histological	Region 3 & 4	279	103.0	2.9
Current study	Histological	Region 3	166	104.5	3.0
Current study	Histological	Region 4	113	101.0	2.7
Sun et al. 2013	Histological	Western PO	258	102.9	
Zhu et al. 2010	Histological	Central Pacific	429	107.8	
Farley et al. 2006	Macroscopic	Southwest PO	299	102.4	2.2
Schaefer et al. 2005	Histological	Eastern PO	683	135.0	

28
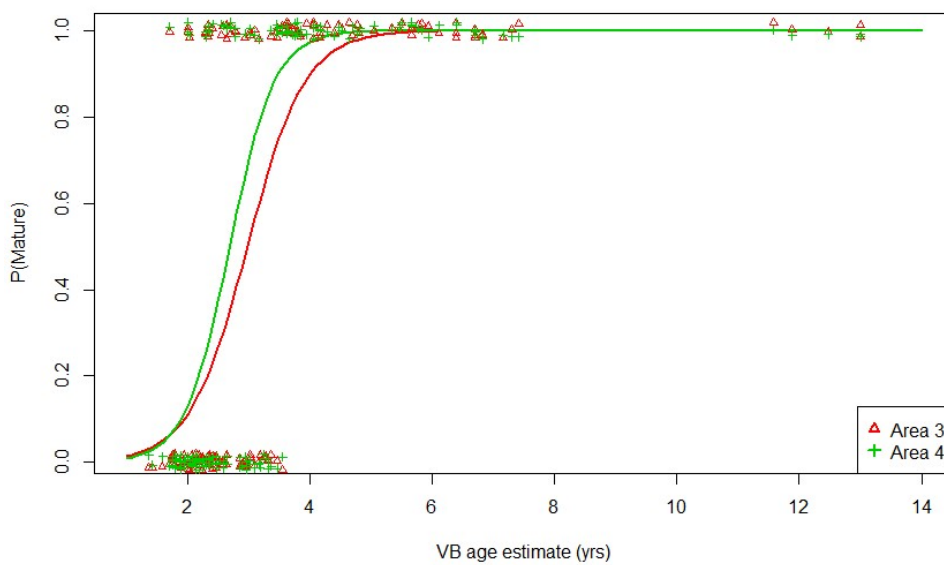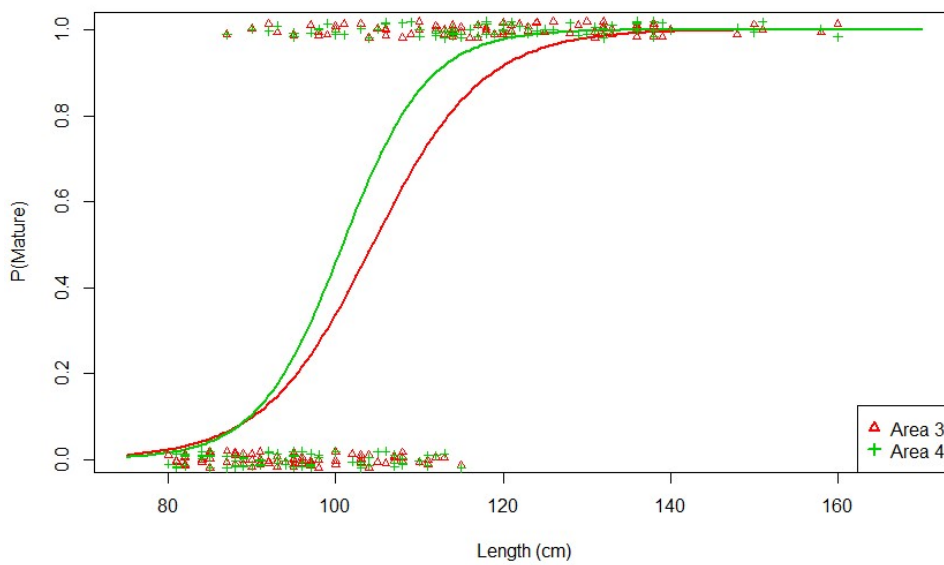
Figure 23. Proportion of mature females by length class (top) and age class (bottom) for regions 3 and 4 combined. L_{50} = 103.0 cm and parameter estimates for length model: alpha = -17.50, beta = 0.17. A_{50} = 2.85 years and parameter estimates for age model: alpha = -6.81, beta = 2.39. Individual mature/immature females are coloured by area and jittered for plotting.

4.3.5 Spatial variation in maturity-at-length/age

Although samples sizes are small for some areas, the results from fitting a logisitic curve to the maturity at length data with latitude x longitude as a 2-dimensional smooth term suggest that maturity varies spatially (Table 9, Fig. 24). The proportion of mature females at a given length tends to increase from the southwest to the northeast of the study region (i.e. the region for which we have samples). This is further illustrated by the predicted maturity at length curves for specified latitude and longitude values (Fig. 24). The lengths at which 50% of the individuals are estimated to be sexually mature (L_{50}) corresponding to these latitude and longitude values are given in Table 10. Note that although the spatial predictions in the top panel of Fig. 24 were calculated for females of length 103 cm (L50 for areas 3 and 4 from the current study; Table 8), this spatial pattern holds true when length is fixed at different values (by necessity since the model did not have an interaction between length and space).

As explained in the Methods, to investigate spatial variation in maturity-at-age we used age estimates calculated from length using the 4 area-specific VB curves derived in the growth analysis (Table 6, Fig. 18). Two of the maturity samples came from area A, 127 from area B, 171 from area C, and 44 from area D (for a total of 342). The correlation between the VB-derived age estimates and the direct (decimal) age estimates is reasonably strong (r = 0.89; Fig. 25).

Similar to the maturity at length results, the results from fitting a logisitic curve to the maturity at age data with latitude x longitude as a 2-dimensional smooth term also suggest that the proportion of mature females at a given length tends to increase from the southwest to the northeast of the study region (Fig. 26). The predicted mean maturity at age curves corresponding to the same latitude and longitude values used in the maturity at length analysis are shown in Fig. 26. The ages at which 50% of the individuals are estimated to be sexually mature (A_{50}) corresponding to these latitude and longitude values are given in Table 10.

Despite the small sample sizes, the larger L_{50} and A_{50} predicted in the southwest (Table 10) suggest that some late-maturing females may remain outside spawning latitudes until mature. Alternatively, these females may be mature regenerating females that were incorrectly classified as immature. This type of misclassification could occur if a fish was caught after spawning was complete and sufficient time had elapsed for the maturity markers to be completely resorbed in the ovary.

Table 9. Summary output from fitting a logistic model to maturity at length data with latitude x longitude as a 2-dimensional smooth term (produced by the summary.gam function in R).

```
Family: binomial
Link function: logit
```

```
Formula:
Status == "Mature" ~ Length + s(Lon, Lat)

Parametric coefficients:
            Estimate Std. Error z value Pr(>|z|)
(Intercept) -18.46863    2.08637  -8.852   <2e-16 ***
Length        0.17716    0.01988   8.909   <2e-16 ***
---
Signif. codes:  0 '***' 0.001 '**' 0.01 '*' 0.05 '.' 0.1 ' ' 1

Approximate significance of smooth terms:
            edf Ref.df Chi.sq  p-value
s(Lon,Lat) 6.573  8.905  36.72 3.06e-05 ***
---
Signif. codes:  0 '***' 0.001 '**' 0.01 '*' 0.05 '.' 0.1 ' ' 1

R-sq.(adj) =  0.579   Deviance explained = 53.8%
UBRE = -0.33194  Scale est. = 1          n = 342
```
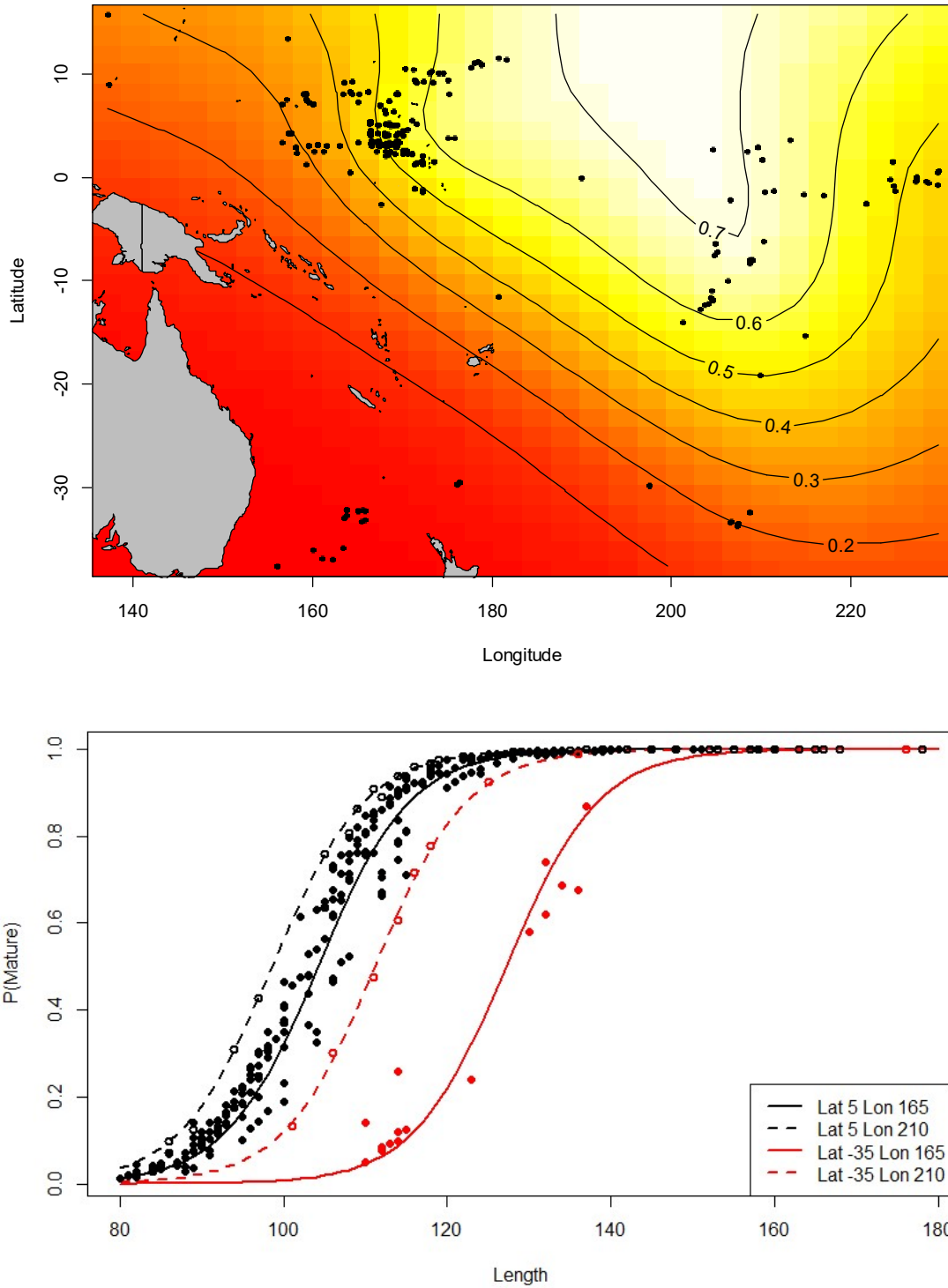
Figure 24. Results from fitting a logistic model to the proportion mature at length data with longitude x latitude as a 2-dimensional smooth term. (Top) Spatial predictions of the proportion of mature females of length 103 cm (L50 for areas 3 and 4 from current study; Table 8); the proportion increases from the southwest to the northeast (red to yellow). (Bottom) Estimated mean maturity at length at specified latitude and longitude values. Points show fitted values. Solid black points correspond roughly to the solid black line (lat>-25, lon<190), open black points to the dashed black line (lat>-25, lon>=190), solid red points to the solid red line (lat<=-25, lon<190), and open red points to the dashed red line (lat<=-25, lon>=190).

Table 10. Estimated length and age at 50% maturity (L$_{50}$ and A$_{50}$) values based on the corresponding latitude and longitude values specified. L$_{50}$ is estimated to the nearest 0.5 cm, and A$_{50}$ is estimated to the nearest 0.05 yrs.

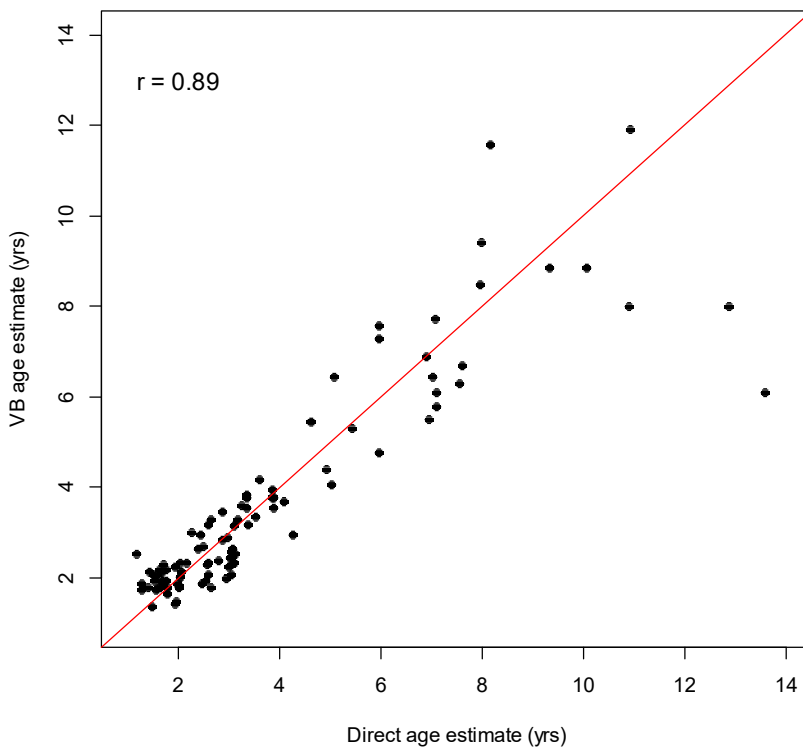| AREA	LAT	LON	L$_{50}$ (cm)	A$_{50}$ (yrs)
Northwest	5	165	104.0	2.95
Northeast	5	210	98.5	2.55
Southwest	-35	165	127.0	5.30
Southeast	-35	210	111.0	3.45

Figure 25. Comparison of decimal age estimates from the otolith data (n=101) with age estimates derived from length using the 4 area-specific von Bertalanffy (VB) growth curves in Fig. 18. The correlation (r) between the estimates is 0.89. The 1:1 line is shown in red.
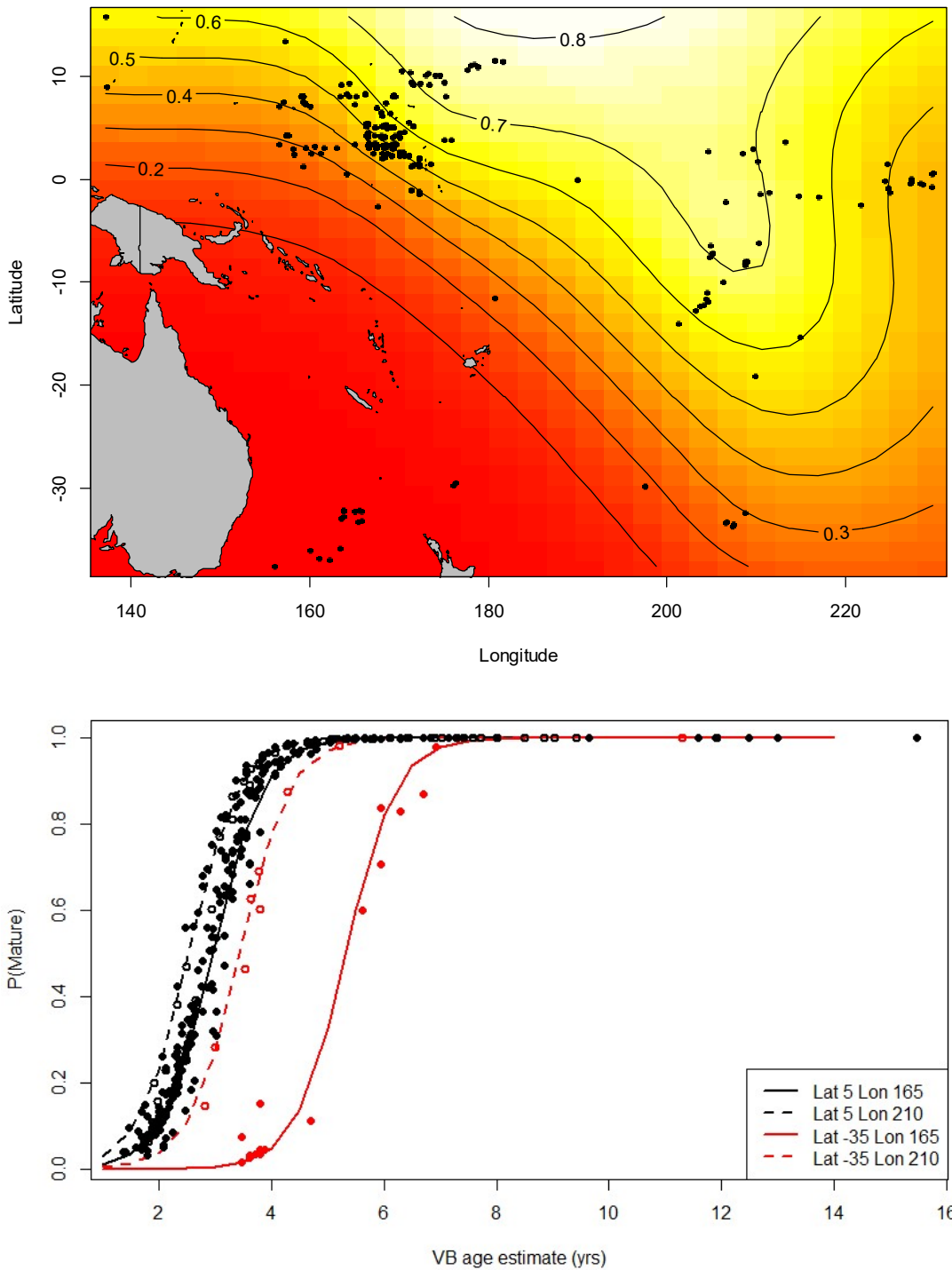
Figure 26. Results from fitting a logistic model to the proportion mature at age data, using age estimates derived from length using the 4 area-specific von Bertalanffy (VB) growth curves in Fig. 18, with longitude x latitude as a 2-dimensional smooth term. (Top) Spatial predictions of the proportion of mature females of age 2.9 yrs (A50 for areas 3 and 4 from current study; Table 8); the proportion increases from the southwest to the northeast (red to yellow). (Bottom) Estimated mean maturity at age at specified latitude and longitude values. Points show fitted values. Solid black points correspond roughly to the solid black line (lat>-25, lon<190), open black points to the dashed black line (lat>-25, lon>=190), solid red points to the solid red line (lat<=-25, lon<190), and open red points to the dashed red line (lat<=-25, lon>=190).

5 Summary

Age and growth

The counts of annual opaque zones from otoliths were precise and reproducible. A direct comparison of microincrements and annual increments verified the location of the first opaque zones in the transverse sections, and the results of marginal increment and edge type analyses were consistent with one opaque zone forming annually. The annual periodicity of opaque zones in sectioned otoliths has been directly validated previously for bigeye in the southwest Pacific Ocean for the age range 2-9 years. (Clear *et al.* 2000; Farley *et al.* 2006).

Microincrements in otoliths sectioned longitudinally were difficult to interpret after 300 zones due to the presence of split zones and zones that merged into each other. We, therefore, recommend caution in the use of length at (daily) age estimates for fish aged >1 year in this study.

We estimated decimal age for bigeye using an algorithm that accounted for birth date, capture date and the state of completion of the marginal increment (edge classification) of the otolith. The maximum estimated age for bigeye in the samples was 13.6 years. We found that annual age (and the VB growth curve) is consistent with the daily age estimates up to age 1. This suggest that the algorithm used to convert annual zone counts to decimal ages daily is reasonable.

The decimal age estimates were used to fit growth curves for male and females, but there was no significant differences in the fits of sex-specific growth models. Similarly, bigeye growth does not appear to vary substantively between regions 3 and 4 of the stock assessment. This result may be influenced by the restricted distribution of samples, as most otoliths were obtained from a small area (20° of longitude) which straddled the two regions.

Additional exploratory work suggested that length-at-age does vary spatially in the WCPO. Further analysis of larger samples size of otoliths from the full size range of fish is required to fully explore spatial variation in growth of bigeye across the Pacific and provide robust growth models. Spatial variation in growth has been demonstrated in albacore tuna in the South Pacific, with greater length-at-age for fish in more easterly longitudes compared to westerly longitudes (Williams et al 2012) and it is reasonable to suspect that region-scale spatial and temporal variation in ocean productivity is likely to impact on rates of growth of tropical tunas.

Reproduction and maturity

A large proportion of the ovaries examined in this study were frozen before being subsampled, fixed and histologically examined. This did not affect our ability to correctly identify histological features, including late stages or atresia/maturity markers and postovulatory follicles, required to accurately classify stages of maturity and spawning activity.

Spawning capable females were caught between 12°N and 12°S. Spawning occurred year-round with indications of peaks in activity in May and October. The SST at all sampling locations north of 20°S was ≥27°C. Spawning capable females were present in SSTs between 27.7 and 30.3°C, but they were in highest relative abundance at SSTs between 28 and 29°C. A large number regressing

and regenerating females were caught in SSTs >27C confirming that not all females are reproductively active in these temperatures.

Estimates of length and age at 50% maturity (L_{50} and A_{50}) for regions 3 and 4 combined were 103.0 cm and 2.85 years respectively. Estimates of L_{50} and A_{50} differed slightly between these regions suggesting that regional variation in maturity may exist. The results of exploratory work also supported the potential for significant spatial variatioin in L_{50} and A_{50} across the region. However, analysis of additional ovaries is required to more comprehensively investigate regional variation in maturity and account for inter-annual variation.

References

Aires-da-Silva AM, Maunder MN, Schaefer KM, Fuller DW (2015) Improved growth estimates from integrated analysis of direct aging and tag–recapture data: An illustration with bigeye tuna (*Thunnus obesus*) of the eastern Pacific Ocean with implications for management. Fisheries Research. 163: 119-126.

Akaike H (1974) A new look at the statistical model identification. IEEE Trans Autom Control 19: 716–723.

Anonymous (2002) A manual for age determination of southern bluefin *Thunnus maccoyii*. Otolith sampling, preparation and interpretation. The direct age estimation workshop of the CCSBT, 11-14 June 2002, Queenscliff, Australia, 39 pp.

Brown-Peterson, NJ, Wyanski DM, Saborido-Rey S, Macewicz BJ, Lowerre-Barbieri SK (2011) A standardized terminology for describing reproductive development in fishes. Marine and Coastal Fisheries: Dynamics, Management, and Ecosystem Science 3: 52-70.

Campana SE (2001) Accuracy, precision and quality control in age determination, including a review of the use and abuse of age validation methods. J Fish Biol 59, 197–242. doi: 10.1006/jfbi.2001.1668.

Chang WYB (1982) A statistical method for evaluating the reproducibility of age determinations. Can J Fish Aquat Sci 39: 1208-1210.

Clear N, Davis T, Carter T (2000) Developing techniques to estimate the age of bigeye and broadbill swordfish off eastern Australia: a pilot study. Final report for Fisheries Research Development Corporation project 98/113, Canberra, Australia.

Farley J, Clear N, Kolody D, Krusic-Golub K, Eveson P, Young J (2016) Determination of swordfish growth and maturity relevant to the southwest Pacific stock. WCPFC-SC12-2016/ SAWP-11.

Farley JH, Clear NP, Leroy B, Davis TLO, McPherson G (2006) Age, growth and preliminary estimates of maturity of bigeye tuna, *Thunnus obesus*, in the Australian region. Mar. Freshw. Res. 57, 713-724.

Farley JH, Davis TLO, Bravington MV, Andamari R, Davies CR (2015) Spawning dynamics and size related trends in reproductive parameters of southern bluefin tuna, *Thunnus maccoyii.* PLoS ONE 10(5): e0125744. doi:10.1371/journal.pone.0125744

Farley JH, Hoyle SP, Eveson JP, Williams AJ, Davies CR, Nicol SJ (2014) Maturity ogives for South Pacific albacore tuna (Thunnus alalunga) that account for spatial and seasonal variation in the

distributions of mature and immature fish. PLoS ONE 9(1): e83017. doi:10.1371/journal.pone.0083017.

Farley JH, Williams AJ, Hoyle SD, Davies CR, Nicol SJ (2013) Reproductive dynamics and potential annual fecundity of South Pacific albacore tuna (*Thunnus alalunga*). PLoS ONE 8(4): e60577. doi:10.1371/journal.pone.0060577.

Hobday AJ, Hartmann K, Hartog J, Bestley S (2006) SDODE: spatial dynamics ocean data explorer. User Guide. CSIRO Marine and Atmospheric Research, Hobart. 8 p.

Morales-Nin, B., 1988. Caution in the use of daily increments for ageing tropical fishes. Fishbyte ICLARM (2): 5-6.

Nicol S, Hoyle S, Farley J, Muller B, Retalmai S, Sisior K, Williams A (2011) Bigeye age, growth and reproductive biology (Project 35). WCPFC-SC7-2011/SA- WP -01

R Development Core Team (2011) R: A language and environment for statistical computing. R Foundation for Statistical Computing, Vienna, Austria.

Schaefer KM, Fuller DW, Miyabe N (2005) Reproductive biology of bigeye tuna (*Thunnus obesus*) in the eastern and Central Pacific Ocean. Inter-Am. Trop. Tuna Comm. Bull. 23, 1-31.

Sun CL, Zeh SZ, Chang YJ, Chang HY, Chu SL (2013) Reproductive biology of female bigeye tuna *Thunnus obesus* in the western Pacific Ocean. J Fish Biol 83: 250-271.

Williams AJ, Farley JH, Hoyle SD, Davies CR, Nicol SJ (2012) Spatial and sex-specific variation in growth of albacore tuna (Thunnus alalunga) across the South Pacific Ocean. PLoS ONE 7(6): e39318. doi:10.1371/journal.pone.0039318.

Williams AJ, Leroy BM, Nicol SJ, Farley JH, Clear NP, Krusic-Golub K, Davies CR (2013) Comparison of daily- and annual-increment counts in otoliths of bigeye (*Thunnus obesus*), yellowfin (*T. albacares*), southern bluefin (*T. maccoyii*) and albacore (*T. alalunga*) tuna. ICES Journal of Marine Science 70:1439–1450.

Wood SN (2011) Fast stable restricted maximum likelihood and marginal likelihood estimation of semiparametric generalized linear models. J R Stat Soc Ser B Stat Methodol 73(1): 3–36. doi: 10.1111/j.1467-9868.2010.00749.

Zischke MT, Farley JH, Griffiths SP, Tibbetts IR (2013) Reproductive biology of wahoo, *Acanthocybium solandri*, off eastern Australia. Reviews in Fish Biology and Fisheries 23:491-506.

Zhu GP, Dai XJ, Xu LX, Zhou YQ (2010) Reproductive biology of bigeye tuna, *Thunnus obesus* (Scombridae), in the eastern and central tropical Pacific Ocean. Environ Biol Fish 88:253–260.

Appendix A: Example images of otoliths prepared for annual ageing.

The first inflection point, each opaque zone and the otolith terminal edge are marked with an x.

BET B5716, 59 cm, unknown sex, increment count 1 Narrow.


BET R4465, 120 cm male, increment count 4 Wide.

BET 4633, 169 cm, male, increment count 12 Narrow.

# Appendix B: Examples of oocyte development classes, postovulatory follicles, atresia and maturity markers from fresh- and frozen-fixed bigeye tuna ovaries.

Oocyte development classes in fresh (left) and frozen (right) fixed bigeye tuna ovaries. A: unyolked (UY). B: early yolked (EY). C: advanced yolked (AY). D: migratory nucleus (MN). E: Hydrated. POF = postovulatory follicle. Scale bar = 500 µm.
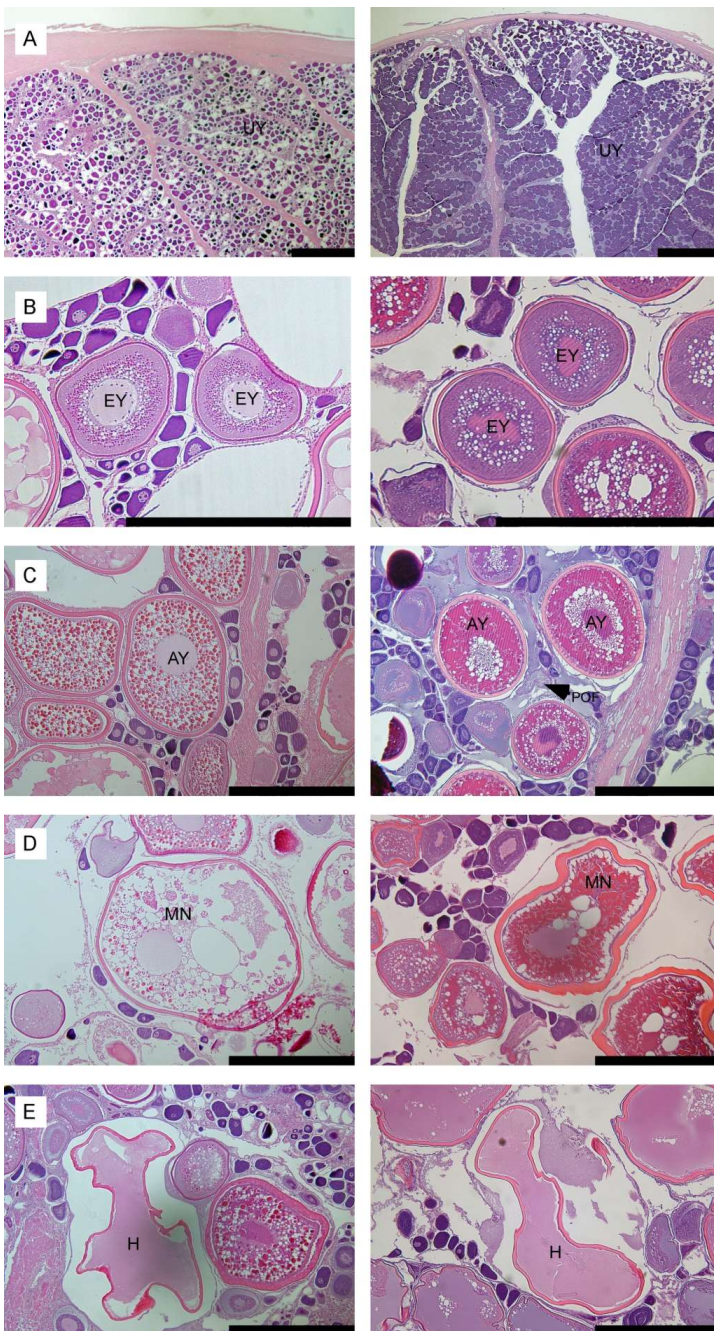
Postovulatory follicles (arrow) in bigeye tuna ovaries. A: POF ~12 hours old in frozen-fixed ovary. B: POF 12-24 hours old in frozen-fixed ovary. C: POF 12-24 hours old in fresh-fixed ovary. Bar equals 100 μm.
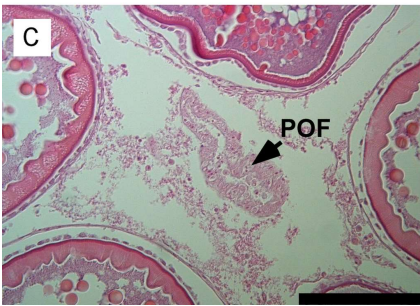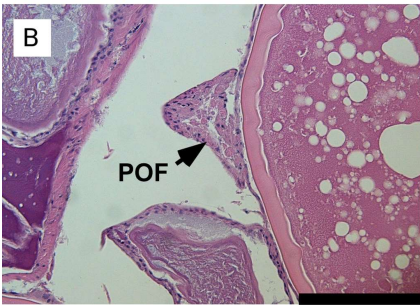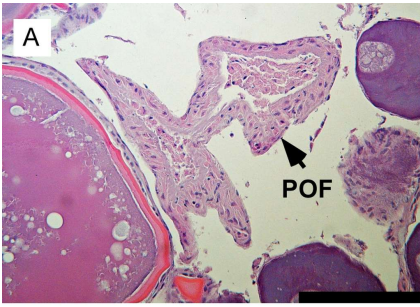
Atresia of advance yolked oocytes in fresh (left) and frozen (right) fixed bigeye tuna ovaries. A: early alpha (α) stage atresia. B = early and late α stage atresia, C: beta (β) stage atresia. Black scale bar = 500 μm; white scale bar = 100 μm.
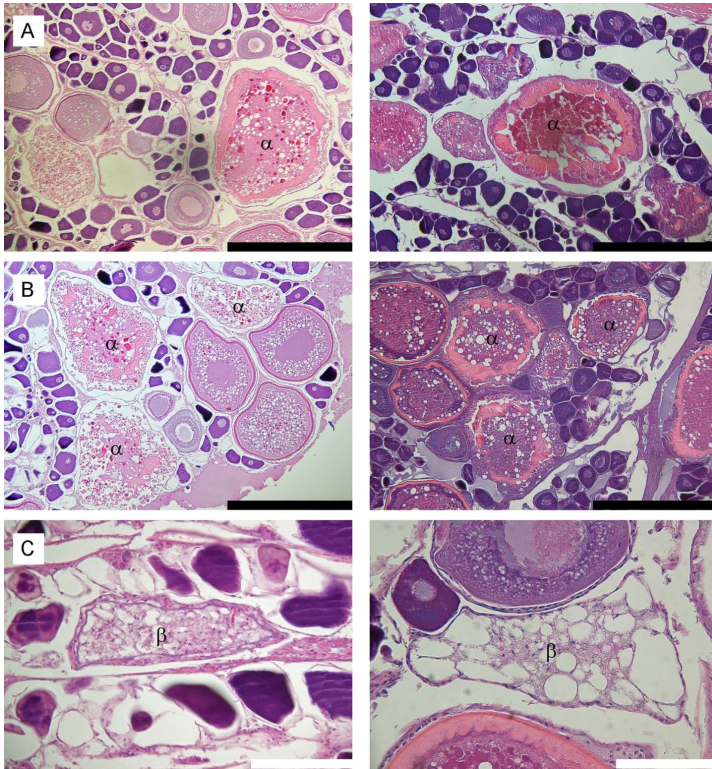
"Maturity markers" in fresh (left) and frozen (right) fixed bigeye tuna ovaries. A: "brown bodies" (black arrows) and unovulated residual hydrated oocytes (RHO). B: "brown bodies" (black arrows). C: clumps of ovulated residual hydrated oocytes (RHO). Black scale bar = 500 µm, white scale bar = 100 µm.
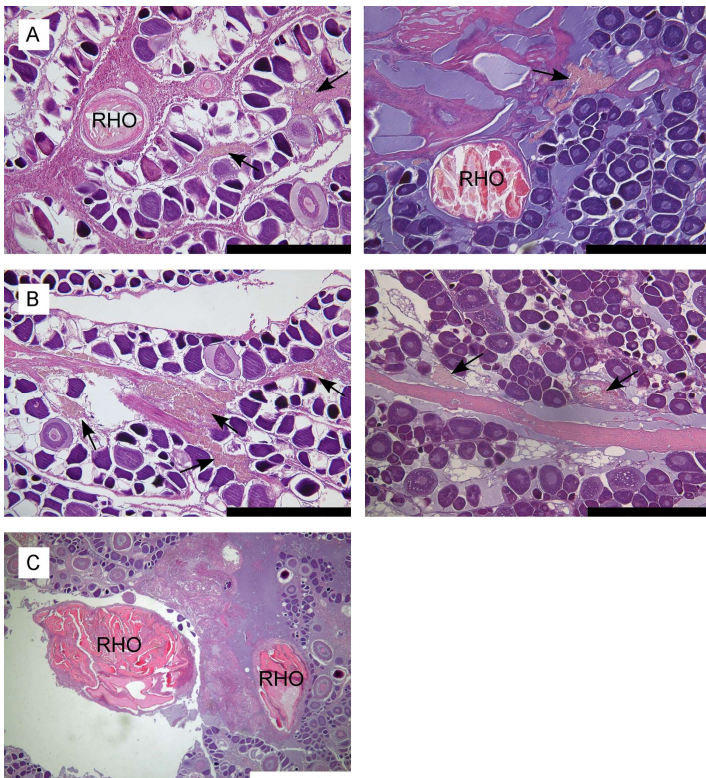
Appendix C: Example image of the otolith from sample B9269 prepared in the longitudinal plain.

Fork length = 83 cm; microincrement count = 457. The arrow marks the general area that microincrement interpretation became difficult.

100µm

Appendix D: Example image of the otolith from sample B12424 prepared in the transverse plain

Fork length = 101 cm; microincrement count = 623. The arrow marks the general area that microincrement interpretation became difficult.

100μm

Appendix E: Example images of otoliths prepared for annual ageing showing variability in length-at-age within and among regions.

Region refers to the regions of the stock assessment (Fig. 1) and area refers to the 4 new areas (A, B, C, D) roughly corresponding to regions of similar growth (Fig. 18). The first inflection point, each opaque zone and the otolith terminal edge are marked with an x. All images are at the same scale.
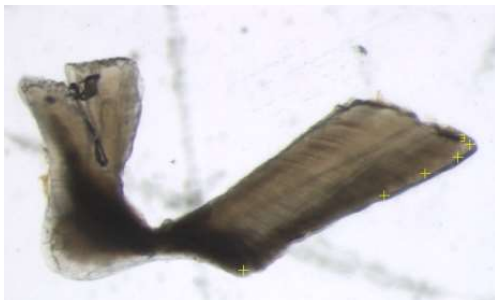
Appendix E.1: Otoliths from bigeye 130 to 133 cm fork length.

FAS14624 Count = 6, age = 6.29 yrs, male
Region 3/ Area B

FAS14619. Count = 5, age 5.31 yrs, male
Region 3 / Area B

FAS14229. Count = 4, age = 3.83 yrs, male
Region 3 / Area B.

FAS14316. Count = 3, age = 3.27 yrs, male
Region 6 / Area C

FAS1704. Count = 5, age = 5.95, female
Region East of 6 / Area D.

FAS14109 Count = 13, age = 13.57 yrs, male
Region 3 / Area B

Appendix E.2: Otolith from bigeye 192 cm fork length.

FAS17020 Count = 11, age = 11.09 yrs, male
Region East of 6 / Area D

Appendix E.3: Otoliths from bigeye 189 cm fork length.

FAS17046 Count = 8, age = 7.88 yrs, male
Region East of 6 / Area D